Integration of multi-archive datasets for the development of a four-dimensional paleoflood model of alpine catchments

Lothar Schulte, Oliver Wetter, Bruno Wilhelm, Juan Carlos Peña, Benjamin Amann, Stefanie B. Wirth, Filipe Carvalho, Antonio Gómez-Bolea

PII: S0921-8181(18)30731-8
DOI: https://doi.org/10.1016/j.gloplacha.2019.05.011
Reference: GLOBAL 2971

To appear in: *Global and Planetary Change*

Received date: 30 December 2018
Revised date: 17 May 2019
Accepted date: 27 May 2019

Please cite this article as: L. Schulte, O. Wetter, B. Wilhelm, et al., Integration of multi-archive datasets for the development of a four-dimensional paleoflood model of alpine catchments, Global and Planetary Change, https://doi.org/10.1016/j.gloplacha.2019.05.011

Integration of multi-archive datasets for the development of a four-dimensional paleoflood model of alpine catchments

Lothar Schulte[1,*] schulte@ub.edu, Oliver Wetter[2], Bruno Wilhelm[3], Juan Carlos Peña[4,1], Benjamin Amann[5], Stefanie B. Wirth[6], Filipe Carvalho[1], Antonio Gómez-Bolea[7,1]

[1]FluvAlps Research Group, Department of Geography, University of Barcelona, E-08001 Barcelona, Spain, schulte@ub.edu

[2]Section of Economic-, Social- and Environmental History & Oeschger Centre for Climate Change Research, University of Bern, CH-3012 Bern, Switzerland

[3]University Grenoble Alpes, CNRS, IRD, Grenoble INP*, IGE, F-38000 Grenoble, France

[4]Meteorological Service of Catalonia, E-08029 Barcelona, Spain

[5]Renard Centre of Marine Geology, Ghent University, B-9000 Gent, Belgium

[6]Centre for Hydrogeology and Geothermics (CHYN), University of Neuchâtel, CH-2000 Neuchâtel, Switzerland

[7]Department of Evolutionary Biology, Ecology and Environmental Sciences, University of Barcelona, 08001 Barcelona, Spain

[*]Corresponding author at: Department of Geography, University of Barcelona, 08001 Barcelona, Spain

Abstract

Both natural and documentary evidence of severe and catastrophic floods are of tremendous value for completing multidimensional flood calendars, as well as for mapping the most extreme riverine flooding phenomena in a river basin, over centennial and millennial time scales. Here, the integration of multi-archive flood series from the Hasli-Aare, Lütschine, Kander, Simme, Lombach, and Eistlenbach catchments in the Bernese Alps constitutes a unique approach to

the reconstruction of flooding events over the last six centuries and to the development of a temporal-spatial model of past flood behavior. Different types of flood archive, be they of natural or anthropogenic origin, record different processes and legacies of these physical phenomena. In this study, paleoflood records obtained from floodplains (four flood series) and lake sediments (four series), together with documentary data (six series), were analyzed and compared with instrumental measurements (four series) and the profiles of lichenometric-dated flood heights (four series) to i) determine common flood pulses, ii) identify events that are out-of-phase, iii) investigate the sensitivity of the different natural archives to flood drivers and forcing, iv) locate past flooding in an alpine region of 2,117 km^2, and v) simulate atmospheric modes of climate variability during flood-rich periods from 1400 to 2005 CE. Asynchronous flood response across the sites is attributed to differences in their local hydrologic regimes, influenced by (i) their physiographic parameters, including size, altitude, storage capacity and connectivity of basins, and (ii) their climate parameters, including type, spatial distribution, duration, and intensity of precipitation.

The most accurate, continuous series, corresponding to the period from 1400 to 2005 CE, were integrated into a synthetic flood master curve that defines ten dominant flood pulses. Six of these correspond to cooler climate pulses (around 1480, 1570, 1760, 1830, 1850 and 1870 CE), three to intermediate temperatures (around 1410, 1650 and 1710 CE), while the most recent corresponds to the current pulse of Global Warming (2005 CE). Furthermore, five coincide with the positive mode of the Summer North Atlantic Oscillation,

characterized by a strong blocking anticyclone between the Scandinavia Peninsula and Great Britain.

For two of the most catastrophic flood events in the Bernese Alps (those of 1762 and 1831 CE), the location and magnitude of all the flood records compiled were plotted to provide an accurate mapping of the spatial pattern of flooding. This was then compared to the pattern of atmospheric variability. The comprehensive 4-D picture of paleofloods thus achieved should facilitate an in-depth understanding of the floods and flood forcing in mountain catchments.

Keywords:

paleoflood; natural flood archives; documentary sources; multi-proxy; Summer North Atlantic Oscillation; Alps

1 Introduction

In a context of global warming and land-cover change, a long-term flood perspective is fundamental for the adequate assessment of hydrological risk in river basins. Both natural and historical evidence (as opposed to extrapolated data) of severe and catastrophic floods are of tremendous value for extending flood calendars so that they can include the most extreme riverine flooding phenomena over centennial and millennial time scales (Baker, 2008; Schulte et al., 2015; Wilhelm et al., 2019). Such field data are able to capture flood dynamics both under different climate conditions during cooler and warmer climate periods (e.g. Medieval Climate Anomaly, Little Ice Age, 20th Century Global Warming) (Büntgen et al., 2011) and during transition periods when storm tracks shifted and atmospheric circulation patterns changed (Mudelsee et

al., 2004; Schulte et al., 2008, 2015; Wilhelm et al., 2012; Peña et al., 2015; Brönnimann et al., 2018). Moreover, they can also undoubtedly mirror the natural forces that prevailed during pre-industrial times. Finally, such data provide a good record of the hydrological imprint of changes in land cover, land use and river management (Böhm and Wetzel, 2006; Schulte et al., 2009a; Wetter et al., 2011; Arnaud et al., 2016).

Different types of flood archives, be they of natural or anthropogenic origin, record the physical phenomena of flooding, allowing the different scientific disciplines to interpret these flood events from their own specific perspectives. Yet, some peak discharges will cause no damage to either property or infrastructure and are not, therefore, recorded in the documentary sources; however, they can lead to flooding and aggradation in floodplains that are recorded in the natural archives. Equally, and more frequently, some floods are not recorded in the natural archives but documentary evidence of the physical damage caused does exist. As such, the spatial and temporal integration of multiple flood data series provides a unique opportunity to compile complete flood calendars, to crosscheck flood series with a considerable degree of accuracy and to develop a temporal-spatial model of past flood behavior for a given catchment or region. The reporting of these individual and integrated paleoflood series to the appropriate public agencies is crucial for the accurate assessment of flood risk. Indeed, local and regional flood information provide a solid foundation for sustained floodplain management that can address society's needs.

One way to assemble paleoflood series is to compare and correlate well-calibrated paleoflood data. Numerous millennia-long flood series have been

reconstructed based on sedimentary, geochemical and botanical proxies retrieved from floodplains, alluvial fans and lakes. Calibration is performed between the occurrence and/or magnitude of well-dated flood deposits in the natural archive and references to extreme events in textual and factual sources. These estimated historical flood magnitudes are in turn calibrated by relatively short-period instrumental data series obtained from gauging stations and by hydraulic modeling (Wirth et al., 2011; Wetter et al., 2011; Jones et al., 2012; Jenny et al., 2014; Corella et al., 2016; Wilhelm et al., 2019). However, multi-proxy approaches of this kind are limited by the fact that the flood data series include only those flood events that lie within the range of sensitivity of the natural archive being examined. The method is based on the assumption that the events calibrated by historical and instrumental series i) define thresholds, frequencies and magnitudes of past floods that occurred prior to the reference periods and ii) represent the (regional) flood dynamics of the studied catchment.

Paleoflood approaches that integrate a greater number (>3) of flood archive types for the same catchment seek to overcome these limitations (Schulte et al., 2015, 2019, this issue). As the gaps in flood series can be identified by comparison, the discontinuities in the flood calendar can be completed by drawing data from the other series. Additional motives for using flood series of different natures are, on the one hand, the ability it affords to plug the hydrological information gap in ungauged catchments (Weingartner et al., 2003; Schmocker-Fackel and Naef, 2010b) and, on the other, to compensate for the paucity of historical data in some regions. This occurs not only in remote areas of low population density or in those of very recent settlement, but also in mountainous headwater catchments.

However, the integration of multi-archive flood records at the regional scale is complex, owing to the statistical processing of non-homogeneous data sets and the correlation of flood series archives of varying dating precision and uncertainties, as well as to the diverse nature of the data, the existence of thresholds (e.g. of erosion and aggradation), the sensitivity of archives and the complexity of processes, varying, for example, between sites of different elevation, catchments of different size, slopes of different exposure and different drainage divides. In short, problems arise from the heterogeneity of catchments and landscapes, whose hydrological and environmental settings differ (Weingartner et al., 2003) and in which the sensitivity of the system to climatological and hydrological extremes can vary depending on the factors controlling river dynamics. This heterogeneous response of the subsystems to flood drivers means that not all flood series can be integrated unthinkingly into a regional paleoflood master curve.

This paper seeks to develop an innovative approach to paleoflood modelling in the main catchments of the Bernese Alps (Switzerland). To do so, it integrates flood data from floodplain and lake sediments and from historical sources with bioindicators from the Hasli Aare, Lütschine, Kander and Simme catchments and the Grimsel, Oeschinen, Iffig and Thun Lakes. By integrating multi-archive flood data into a master curve, periods of higher paleoflood frequency over the last 600 years can be identified and atmospheric circulation modes during flood-rich periods can be simulated using the paleo-climate sea-level pressure (SLP) grid developed by the Last Millennium Ensemble (LME) project.

Finally, the paper shows that a multi-archive approach makes it possible to analyze the 3-D spatial distribution (horizontal and vertical) of flood records over

long time scales (4-D) and to capture the physiographic and environmental diversity of catchments, as well as the variability and forcing of floods in mountain regions, much better than when employing a single record type.

2 Regional Setting

The morphology of the Alpine Aare basins (46°41'N, 6°04'E; Figure 1), situated on the northern slope of the Swiss Alps, is dominated by alpine limestone landscapes to the north and west and by alpine crystalline landscapes to the south and east. The study area is subdivided into four headwater catchments: the Hasli-Aare (596 km^2), the Lütschine (379 km^2), the Kander (496 km^2) and the Simme (594 km^2). The study also includes two smaller catchment tributaries: the Lombach (48 km^2) and the Eistlenbach (4 km^2), lying to the north.

The geology of the Aare catchment is structured by SW-NE thrust faults that define the spatial distribution of its main tectonic units. The north-western area includes flysch, limestone, and marls of the Mesozoic Penninic nappes, siliceous limestone of the Ultrahelvetic domain and carbonate rocks of the Helvetic nappe. To the south, this area is bounded by the Infrahelveticum, a narrow band of sandstone-rich flysch and limestone. The central area of the Hasli-Aare and Lütschine basin belongs to the Aare massif. From north to south, the para-Mesozoic bedrock includes granite, gneiss and micaschist. The southern area of the Hasli-Aare catchment is formed by old basic-ultrabasic crystalline rocks and late Paleozoic intrusive rocks form the highest slopes and summit areas in the Aare Massif, reaching up to 4274 m a.s.l. (Finsteraarhorn).

The geomorphology of the Bernese Alps includes complex connected Pleistocene glacial landforms and Holocene heterogenic alpine landforms, such as cirques, glacier forefields, moraine walls, overdeepened valleys, scree slopes, and alluvial cones. Other landforms, such as rock avalanches, result from the non-linear threshold dynamics of the interglacial adaptation cycle. In contrast, some landforms, such as moraines, alluvial fans, alluvial plains and deltas, are sensitive to deposition controlled by intracentennial climate variability. Average sedimentation rates of the Hasli-Aare flood plain range from 2.02 to 6.52 mm yr^{-1} (Carvalho and Schulte, 2013) while those of the Lütschine delta floodplain range from 1.58 to 1.91 mm yr^{-1} (Schulte et al., 2004).

Lake Brienz, with an altitude of 564 m a.s.l., defines the base level of erosion of the Hasli-Aare and Lütschine river systems. The downstream end of the Hasli-Aare catchment comprises a 12-km long and 1-km wide delta plain (Fig. 1), whereas the Lütschine river system accumulated a 4-km long fan delta which separates Lake Brienz from Lake Thun.

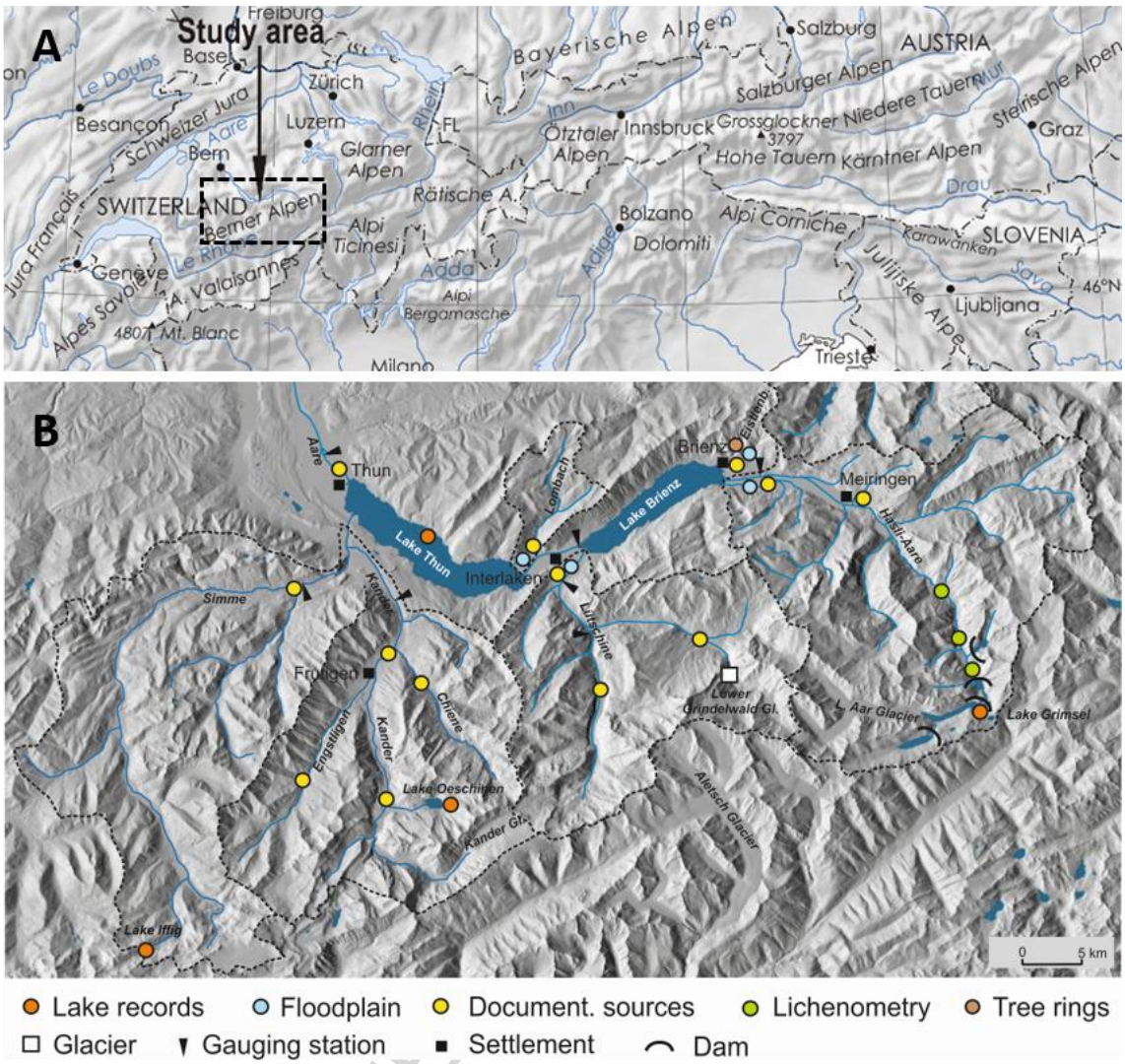

Catchment	Type of archive	Catchment (km2)	Elevation record (m a.s.l.)	Highest elevation (m a.s.l.)
Lake Thun	Lake, historical	2451	558	4273
Hasli-Aare	Fluvial, hist., instr., lichen, lake Grim.	596	568	4273
Simme	Historical, instr., lake Iffig	594	663	3243
Kander	Historical, instr., lake Oes.	496	646	3698
Lütschine	Fluvial, hist., instr.	379	569	4158
Lombach	Fluvial, hist.	48	569	2085
Lake Oeschinen	Lake	21	1580	3661
Lake Grimsel	Lake	5	1908	2941
Lake Iffigsee	Lake	4,6	2065	3246
Eistlenbach	Fluvial, hist., tree rings	4	644	2204

Figure 1: A) location of the study area in the Alps. B) Shaded relief, location and type of flood archives (dots) mentioned in text and metadata (table below) of catchments studied in the Bernese Alps. Digital elevation model was provided by Swisstopo. Table: List and characteristics of the studied catchments.

At 558 m a.s.l. Lake Thun (-5 m lower than Lake Brienz) is the base level of erosion of the Kander river and the smaller Lombach stream, whereas the Simme River flows into the Kander River at Reutingen, 4 km upstream of the delta. Before 1714 CE, the Kander flowed directly into the Aare River to the north, approximately 6 km downstream from the outflow of Lake Thun. Subsequent to the river diversion in 1714 CE, one of the earliest river correction projects to be undertaken in Switzerland, the Kander River caused massive incision upstream due to the steepening of its longitudinal profile (Vischer, 2003).

The floodplain morphology of the Lower Hasli valley, the Lütschine and the Lombach fan deltas presents fluvial landforms, including paleochannels, levees, crevasse splays, and interdistributary basins. According to the stratigraphic units studied in sections and cores, layers of fluvial gravel, sand, and silt intertongue with organic-rich beds and peat horizons, which result from wetland environments with a high water table. The floodplains of the Kander and Simme Rivers are narrower than the Hasli-Aare valley. Floodplain sediments are coarser due to the contribution of side-valley tributary fans, leading to upstream incision.

The small Eistlenbach torrent has formed an alluvial cone. This is blocked at its distal front by a bedrock ridge, which has forced the resulting drainage system to the west. Accommodation spaces between the alluvial cones are ideal traps for differentiated aggradation of mostly sand, silt, and clays which alternate with organic and peat horizons.

The four lakes studied here (Grimsel, Iffig, Oeschinen, and Thun) originate from glacial overdeepening. Today, 30% of the Oeschinen catchment is glaciated.

However, during the Little Ice Age, Lake Grimsel and Iffig were also fed by meltwater from cirque glaciers, as documented by the historical Maps of Meyer and Weiss (1797), Dufour (1845-1865) and Siegfried (1880). All these lakes act as sediment traps for the material transported by mountain streams during flooding, forming flood layers that are preserved in time at the bottom of the lake basin: Lakes Grimsel, Iffig and Oeschinen in small, high-elevation catchments and Lake Thun at the bottom of the main valley integrating the signal of all sub-catchments.

In the northern Bernese Alps, floods have been triggered mainly by precipitation anomalies, such as intensive summer thunderstorms and long-lasting advective rainfall events, combined with pronounced snowmelt as well as glacier lake or landslide-dammed lake outburst floods (Röthlisberger, 1991; Gees, 1997; Weingartner et al., 2003; Peña et al. 2015). According to the 500-year historical flood record of the Aare River (Schulte et al., 2015), 95% of the floods occurred during the summer months of July and August. In the study area, the annual mean precipitation ranges between 1175 mm yr^{-1} at Interlaken, on the Lütschine delta, to around 2800 mm yr^{-1} at the summit level of the Aare massif (MeteoSchweiz, 2014).

According to the instrumental hydrological data recorded in the Bernese Alps since 1905, the hydrological regime of the main rivers ranges from glacial (Aare, Lütschine; 17% of the catchment area is covered by glaciers) and glacial-nival (Kander) to nival (Simme). The mean annual discharges reach 35 $m^3 s^{-1}$ in the Aare basin at the Brienz gauging station, 18 $m^3 s^{-1}$ in the Lütschine basin at Gsteig, 41 $m^3 s^{-1}$ in the Kander basin at Hondrich and 36 $m^3 s^{-1}$ in the Simme basin at the Latterbach station.

In the Bernese Alps, periods of increased land-use have been recorded since the Bronze Age (Schaer, 2003; Guyard et al., 2007; Ebersbach et al., 2010). As floods and debris flows are the main natural hazards in the region, local communities have developed various adaptation and mitigation strategies over the centuries. For example, the oldest buildings (dating back to the 15th century) are often located on distal areas of alluvial cones, on the opposite side of the alpine streams or on bedrock ridges and trough shoulders. In traditional rural areas (those less influenced by tourism), these strategies still form part of the cultural landscape and its settlement patterns.

Since the Kander was diverted to Lake Thun in 1714 CE (Vischer, 2003), many stretches of the Aare, Lütschine, Lombach, and Kander Rivers have been channelized, especially during the 19th century. Since 1932 CE, reservoirs built to generate hydroelectric power have had a varying influence on the flood dynamics of the Hasli-Aare catchment, depending on their retention capacities.

According to the 2017 CE census, a total of 69,328 inhabitants reside in the study area: 8,611 in the Hasli-Aare, 21,651 in the Lütschine, 6,243 in the Lombach, 15,757 in the Kander and 17,066 in the Simme catchments. Furthermore, the population densities of the municipalities in these valleys are among the highest per productive area in the Alps, ranging from 25 to 100 inhabit. km^{-2} to maximum values of 250-1000 inhabit. km^{-2} on the Lütschine and Lombach fan deltas and along the western shoreline of Lake Thun. In contrast to the nearby Lütschine delta, no towns or villages are located on the Hasli-Aare floodplain. A similar pattern can also be observed in the Kander valley, with the exception of some districts of Frutigen. Due to demographic pressure during the 19th and 20th centuries and as a result of the development of grazing,

agriculture, forestry, tourism and infrastructure, and the introduction of hydraulic management of the floodplains, present-day human activities (e.g., tourism) are not limited to traditional low-risk areas.

3 Data and Methods

The northern slopes of the Bernese Alps were selected as our pilot study area because of their high flood data density and because of the rich diversity of natural archives, documentary evidence and instrumental data available, the result of the intense research activity conducted on these slopes by various research groups over the last decade. For example, the University of Barcelona's FluvAlps Research Group has compiled flood proxies from the sedimentary, geochemical, botanical and geomorphological data, as well from textual and factual sources and from the instrumental data from the area's floodplains (Schulte et al., 2004, 2008, 2009a, 2009b, 2015). The Environmental History and Historical Climatology Group at the Oeschger Centre for Climate Change Research (University of Bern) has archived historical flood data from the Aare, Kander and Simme Rivers (Wetter, data collection). The Paleolimnology Group at the University of Bern has conducted studies on Lake Oeschinen aimed at reconstructing past warm season precipitation and flood frequency variability (Amann et al., 2015), while the Geological Institute at ETH Zurich, the Sedimentology Group at EAWAG and the Quaternary Science and Paleoclimatology Group (University of Bern) have studied flood frequency across the central Alps by analyzing 15 lake records, including those of Grimsel, Iffig and Thun (Wirth et al., 2011, 2013; Glur et al., 2013).

The present paper draws on published historical and paleoflood data as well as on a number of unpublished flood series provided by the authors and/or research teams that have participated in this project. The team of authors agreed to use these unpublished data (which are to appear in free-standing papers currently under preparation) to improve our evidence of past flood events in the Bernese Alps and so as not to delay unnecessarily the publication of this paper. These unpublished datasets are clearly identified in the text, figures and tables.

Figure 1 shows the shaded relief digital elevation model of the study area, identifies the catchments and watersheds and reports the location and type of flood archives. It also provides key metadata listing the size of the catchment areas, the altitude of the flood records and the highest catchment elevations. All the flood records mentioned in this paper are depicted in the map included as Figure 1. Some flood records were not selected for integration (see section 5) because the series show either i) poor data density (the case of documentary data from the Simme River), ii) low or changing resolution of proxies (e.g. Lake Iffig and Grimsel and the Lütschine flood plain), or iii) strongly human influenced or disturbed series (e.g. the sedimentary records of the Lombach delta flood plain over the last 900 years). Other records, such as the lichenometric data of flood levels in the higher Hasli-Aare catchment and the dendromorphological data from trees on the Eistlenbach fan, were used to support flood proxies. The reconstructed and measured lengths of the Grindelwald glacier were used as a paleoenvironmental proxy for comparison. In addition to their use in the flood model, all archives were used to compile the spatial distribution of flooding evidence in the maps included in section 7.

The number, type and setting of the flood archives present marked differences from one alpine catchment to another. Thus, from the large Hasli-Aare catchment (596 km^2), sedimentary paleoflood series were constructed from Lake Grimsel and from the Hasli-Aare floodplain; lichenometric dating of flood levels was conducted along the higher stretch of the Hasli-Aare; textual and factual historical flood damage data are found referring to the lower Hasli-Aare floodplain; and discharges were measured at the Brienzwiler gauging station. In the Lütschine catchment (379 km^2), flood data were obtained from delta floodplain sediments, documentary sources and discharge measurements at the Gsteig gauging station. Flood data from the Kander catchment (496 km^2) include the flood layers of Lake Oeschinen, historical flood damage data from the valley and instrumental flood records from the Hondrich gauging station. The data from the large Simme catchment (594 km^2) are not as extensive and include only the flood layers of Lake Iffig and instrumental records from the Latterbach gauging station. The records from Lake Iffig include far fewer flood layers than those of Lake Oeschinen and the documentary archives for this catchment have not yet been studied in sufficient detail. This suggests that more information could potentially be extracted in the future. In the case of Lake Thun, a 160-year young sedimentary flood series, which can be compared to the floods of the Kander and Simme catchments, was constructed by Wirth et al. (2011) using several sediment cores taken from different locations in the deep lake basin. As for the smaller northern Aare tributaries, data from the Lombach catchment (48 km^2) include sedimentary and geochemical flood proxies, but only for the period 2300 to 1100 cal yr BP. In contrast, excellent geochemical data were obtained from the distal basin of the alluvial cone fed by

the small Eistlenbach catchment (4 km^2) from 3200 yr cal BP to present, historical fluvial landforms were dated by tree rings (data not shown) and historical flood data were provided by the Cantonal Office of Forest (KAWA) and from Schneider (2010).

In the following subsections of section 3, the data and methods used in this study (Figure 2) are presented according to each flood archive type.

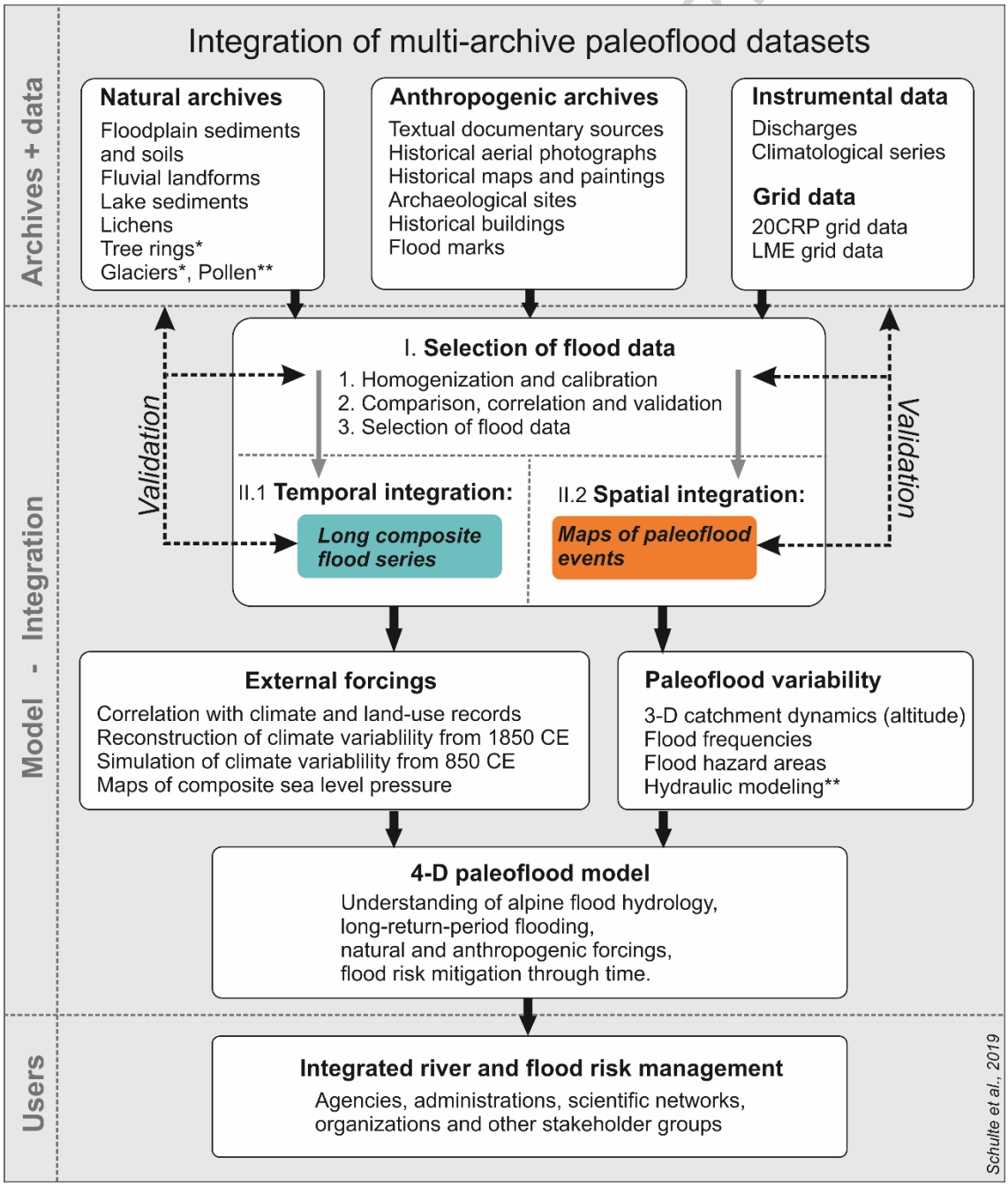

Figure 2: Conceptual scheme for the integration of multi-archive datasets for the development of a four-dimensional paleoflood model of alpine catchments. * Records referred to only occasionally in this paper. ** Records used in project but not presented in this paper.

3.1 Geoarchives from delta floodplains

In recent decades, several studies have been conducted aimed at reconstructing the frequency, magnitude and provenance of paleofloods from the sedimentological and geochemical signature in floodplain deposits (Schulte et al., 2008, 2015; Jones et al., 2012; Berner et al., 2012). In this paper, sedimentary archives and morphological evidence of floods (Figure 1 and 2) are included from the floodplains of the Lütschine (Schulte et al., 2004, 2008, 2009a) and the Lombach fan delta (Schulte et al., 2009b), the floodplain of the lower Hasli-Aare delta (Carvalho and Schulte, 2013; Llorca et al., 2014; Schulte et al., 2015) and from a marginal basin of the Eistlenbach alluvial cone (Schulte et al., 2016).

Meso-scale fluvial structures were mapped by geomorphological survey and the analysis of historical maps (from the 16th century onwards), aerial photographs (1928-1944), IR and SPOT images (2005), and a 2-m spatial resolution digital terrain model (2005). Here, our objective was to understand the spatial and temporal development of the fluvial landforms, including floodplains, deltas, fan deltas, and alluvial cones, and, as a result, to select appropriate core sites.

To investigate the lithostratigraphic aggradation units, exposures were described and sampled, and percussion coring with an open liner was conducted along transversal and longitudinal transects, reaching a maximum depth of 17 m. At strategic sites, 1-m long closed cores were recovered from depths of up to 11 m. The best sedimentary and geochemical proxy data were obtained from floodplain deposits retrieved from intradistributary and marginal

basins, where overbank flood deposits were trapped in relatively calm palustral depositional environments. Organic soil and peat formation dominate periods of diseased flooding.

The chronological models of section profiles and cores are based on i) calibrated radiocarbon dating of peat, plant remains, wood, and charcoal; ii) ^{210}Pb dating; iii) optically stimulated luminescence dating, iv) artifacts, and v) correlation of marker horizons (Schulte et al., 2009, 2015). Modern historical flood layers were compared and calibrated with documentary flood evidence and global geochemical signals (e.g. Pb and Zn trends). The age of each core sample was linearly interpolated.

The provenance, deposition and diagenetic processes of materials and pedological features were investigated by macroscopic description and microscopic identification in thin sections. Analysis of chemical elements was performed by XRF-core scanning (AVAATECH) at 1-cm intervals and calibrated by conventional X-ray fluorescence (XRF) of pearls. Total organic carbon (TOC) and grain-size fractions were measured at 1-cm intervals.

To generate environmental proxies from delta plain sediments, the geochemical variability of the core samples was analysed employing the following procedure (Schulte et al., 2008, 2015): i) series of individual elements were plotted versus lithology, grain size and TOC along with sample depth, ii) elements were analysed as Ti ratios to remove possible alterations in XRF-scan intensities, iii) factor analysis (FA) was computed to explore the variability of the geochemical data sets, iv) the Zr/Ti, Sr/Ti, and Ca/Ti ratios were compared with grain-size fractions to produce grain-size flood proxies, and v) the frequency of flood

layers and Zr/Ti peaks were compared to the historical flood index reconstructed from documentary sources.

Of the four catchments presenting sedimentary and geochemical floodplain proxies, the Hasli-Aare delta floodplain and the Eistlenbach marginal basin were selected for the flood series integration because they cover the period 700 to 2005 CE, and above all the period after 1400 CE, at a suitably high resolution. The floodplain proxies of the Lütschine catchment and the Lombach fan delta were not integrated because they present low sedimentation rates over the last 900 years.

3.2 Geoarchives from lakes

In recent decades, techniques have been developed for reconstructing long paleoflood series based on the identification and dating of detrital layers resulting from flooding and which are embedded in lake sediment sequences (Gilli et al., 2013; Schillereff et al., 2014; Wilhelm et al., 2018, 2019). The present paper includes paleoflood data originating from the study of four lake sediment sequences in the Bernese Alps (Figure 2): namely those of the Grimsel (Glur et al., 2013), Iffig (Glur et al., 2013; Schwörer et al., 2014), Oeschinen (Amann et al., 2015) and Thun Lakes (Wirth et al., 2011; Figure 1). These lakes are located along an altitudinal transect with the high-elevation lakes of Grimsel (2941-1900 m a.s.l., 5 km^2), Iffig (3246-2065 m a.s.l., 4,6 km^2), and Oeschinen (3661-1580 m a.s.l., 22 km^2), as well as Lake Thun (560 m a.s.l., 2500 km^2) located in the valley of the Aare River. The geology of the Iffig and Oeschinen catchments is dominated by sedimentary rocks, while crystalline

rocks dominate in the Grimsel catchment. Extending over a much larger area, the geology of the Lake Thun catchment is characterized by various lithologies that include both crystalline and sedimentary rocks. The land cover of the three high-elevation lake catchments comprises alpine meadows (under pasture in the Lake Iffig catchment) and scree slopes. Today, the catchments of Lakes Oeschinen, Iffig and Thun (9.5% in 2008) are still glaciated, reaching 30% in the case of the Lake Oeschinen catchment area.

For all lakes, sediment cores were retrieved from the deepest parts of their basins, where the sediment sequences, including the flood layers, are well preserved. Flood layers are usually characterized by a mineralogical composition that reflects the catchment's geology, a coarser grain size than is typical given the background lake sediments, one or several fining-upward sequences, and terrestrial organic matter. For all lake sequences, flood layers were first identified by macroscopic observations.

In addition, laser grain-size analyses were undertaken in the Oeschinen and Thun lakes to support flood-layer detection. The higher river energy during flooding is reflected by the coarse grain sizes of the flood layers while the grain-size evolutions within the layers reflect the hydrodynamics of the floods (i.e. coarsest grain size transported during the flood peak). Complementary measurements of the physical characteristics of the retrieved cores, performed using a GEOTEK multi-sensor core logger (gamma-ray attenuation bulk-density, magnetic susceptibility) with a 5-mm sampling step, were also used for the Grimsel, Iffig and Thun sediment sequences. These measurements help detect flood layers characterized by both a higher density and a higher concentration of heavy minerals compared to the sedimentary background.

Microscopic observations of thin sections were also performed on the Oeschinen sequence to identify flood layers at the sub-mm scale.

Short-lived radionuclides (^{137}Cs on all sequences and ^{210}Pb on Oeschinen sequence only) were measured to date the most recent part of the sequences, while radiocarbon (^{14}C) dating was used on terrestrial macro-fossils for the older parts. For the Grimsel and Iffig lakes the ^{14}C age-model uncertainty (i.e. beyond the ^{137}Cs zero activity at 1950 CE) for the past 500 years is ±15 to 79 and ±9 to 60 years, respectively. As the Oeschinen sequence presents varved sediments (annual laminations), the counting of laminae on thin sections allowed high-resolution dating of this sequence within an uncertainty ranging from 2 years for recent deposits to 30 years for the oldest. Site descriptions and details about the methodologies applied and the results obtained for the detection of flood layers and their dating can be found in Wirth et al. (2011; Lake Thun), Glur et al. (2013; Lakes Grimsel and Iffig), Schwörer et al. (2014; Lake Iffig) and Amann et al. (2015; Lake Oeschinen).

3.3 Documentary and instrumental flood series

Even though the valleys of interest to us here are quite highly populated, the regional setting of the Bernese Alps is much less favorable for undertaking historical, documentary evidence-based hydrological analyses – compared, that is, to the Circum-Alpine cities – essentially because of the significantly poorer availability of documentary data. However, thanks to a significant amount of preparatory groundwork (historical hydrological flood data collected by Wetter, unpublished; Lohner, 1864; Lanz-Stauffer and Rommel, 1936; Röthlisberger,

1991; Graf, 1991; Beeli, 1998; Pfister, 2006; Hügli, 2007; Bütschi, 2008, Euro-Climhist www.euroclimhist.unibe.ch), it has been possible to compile long-term historical documentary flood evidence series with an acceptable data density (Figure 1 and 2), in part, dating back to the 15th century for the Rivers Hasli-Aare (Schulte et al., 2015), Lütschine (Schulte, unpublished), Kander (this paper) and the Aare from Thun to Bern (Wetter data collection, unpublished).

The historical documentary evidence that includes reports about flood events makes reference to the following settlements: Meiringen, Innertkirchen, Guttannen, Nessental and Gadmen in the Hasli-Aare catchment; Kandertal, Kandersteg, Kandergrund, Mülenen and Frutigen/Äschi in the Kander catchment; Lütschenental, Zweilütschinen, Lauterbrunnen, Wilderwil, Bönigen, Matten and Interlaken in the Lütschine catchment; Lenk, Niedersimmental, Obersimmental, Simmental, Reutigen in the Simme catchment; the city of Thun at the Aare's outflow from Lake Thun; and the villages between the cities of Thun and Bern on the floodplain of the pre-alpine Aare River). Documentary flood data of the Eistlenbach brook, which date back to the 18th century, were obtained from the village of Hofstetten. Only the historical documentary evidence for the Simme River has yet to be analyzed by a trained historian, suggesting that more relevant flood data could well be extracted in the future. Information about flood events since 1973 CE were completed with details from the Swiss flood and landslide damage database maintained by the Swiss Federal Institute for Forest, Snow and Landscape Research and were crosschecked with regional precipitation data from the IDAWEB data bank of Meteoswiss.

To estimate historical flood intensities between 1408 and 2012 CE, primary and secondary indications of flood classifications were defined according to the scale of damage and geomorphic change. Although various flood classifications and typologies have been proposed (see, for example, Röthlisberger, 1991; Pfister, 1999), in the present study we adapted our flood criteria to the local physiographic, socio-economic and demographic settings of the Aare, Lütschine, and Kander catchments (Schulte et al., 2015; Wetter flood data collection, unpublished). Based on these criteria, magnitudes were assigned to documentary evidence-based historical floods, damage from tributaries was incorporated (with their corrected weight) and flood indices were plotted for each basin (Figure 6). Because the precision and continuity of historical flood data series change over time – information about small and medium flood categories before 1850 CE being particularly limited – only flood events M>1.5 were integrated. Flood frequencies were plotted separately for the alpine catchments (Hasli-Aare, Lütschine, Kander and Simme Rivers) and for the pre-alpine Aare river stretch from Thun to Bern and, then, both were smoothed with a 31-yr and 81-yr Gauss filter (Figures 6 and 9).

Instrumental discharge measurements (annual maxima) have been recorded at the Thun station on the Aare River (660 m downstream of Schwäbisbrücke) since 1906 CE. This instrumental series was extended using reconstructed documentary evidence based on flood levels at the town of Thun (Rathausplatz) dating back to 1714 CE. The water levels recorded in the instrumental series were then linearly corrected to the reference location of the documentary evidence, i.e. the Rathausplatz. The instrumental measurements for the River Kander were first recorded in 1902 at the Hondrich station (0/00307), which was

relocated to its present site in 1980. The Gsteig station on the Lütschine River and the Brienzwiler station on the Hasli-Aare have been operative since 1908 and 1903, respectively.

3.4 Lichenometric dating of flood levels

In the higher Hasli Valley, lichen thalli measurements (in line with Armstrong, 2016) were taken on the crustose lichens *Rhizocarpon macrosporum* and *Rhizocarpon geographicum ssp. frigidum* to estimate the age of exposure of crystalline rock faces after floods (Figure 1 and 2). The approach is based on the prerequisite that turbulent floods erode the exposed surfaces "cleaning" off the lichen thalli and that, subsequently, new lichen colonization starts on the resistant rock surface. Thus, the measurement of the largest individual lichen or groups of isometric lichens at different altitudes provides information to reconstruct the height of past flood levels along a topographic cross-section (Figure 8). From the measurement of the thalli of 93 lichens on surfaces of known age – including, gravestones, buildings, bridges, and road sections in the municipalities of Guttannen, Meiringen, Wilderswil and Innertkirchen – a calibration curve for the Bernese Alps (Losada et al., 2014) was constructed, providing us with a regional radial growth rate of 0.52 mm a^{-1}. Dating uncertainties range within an interval of 2-10% (decreasing with age). Major errors are introduced by a delay in colonization and the possible disturbance of vegetation and soil cover. Forty-four lichenometric ages were obtained along four cross-sections in the higher Hasli-Aare gorges, where the river cuts into plutonic bedrock. Finally, the ages of the different flood levels were compared

with historical flood data from the Lower Hasli valley and considered correct when recorded, at least, in two lichenometric sections.

3.5 Integration of multi-archive flood series

The integration of the multi-archive flood series was performed by means of a complex procedure comprising two stages (Figure 2): in the first, flood series from different locations and different archive types were processed, analyzed and compared, and, in the second, flood series were integrated into a flood master curve that covers the period from 1400 to 2005 CE.

The first stage began with the selection and preparation of the available flood data series (Figure 2). Sedimentary and geochemical floodplain proxies were plotted alongside each other and filtered. Visual correlation of 12-year averaged floodplain records and climate proxies from tree rings (Büntgen et al., 2011) was performed to define flood periods and a spectral analysis was performed to investigate flood frequencies (Schulte et al., 2015).

To compare the flood records of Lakes Oeschinen, Iffig, Grimsel and Thun, frequencies of occurrence and thicknesses of flood layers were plotted according to the age models. Because the sedimentation rates and sensitivity tests show marked differences between the lake records and the historical Kander flood index, thresholds of >7 mm and >9.5 mm flood layer thicknesses were applied to the Lake Oeschinen flood data, the record presenting the highest resolution. Subsequently, the filtered Lake Oeschinen flood record was plotted against the documentary Kander flood series to test whether the major flood events coincided. Additionally, lake flood data series were smoothed using

an 81-yr Gauss filter (filter adopted to match the frequency of the Gleissberg solar cycle) to compare major flood frequency trends.

The historical flood damage indices of the Hasli-Aare, Lütschine, Kander, and Simme Rivers were plotted alongside each other and flood clusters were identified. Floods with magnitudes M>1.5 in these four alpine catchments were then integrated into one historical alpine flood curve that was smoothed using a 31-yr running Gaussian filter. The same procedure was applied to the pre-alpine Aare documentary flood archive, which records flood damage along the river stretch between the cities of Thun and Bern. The flood trends of the integrated alpine Aare catchments were compared with those of the pre-alpine Aare River to identify common flood periods.

Annual peak discharge measurements from the Brienzwiler gauging station were compared to historical flood magnitudes and geochemical floodplain proxies of the Hasli-Aare catchment. Likewise, in the Kander catchment, the instrumental data from the Hondrich station were compared with the flood records in the documentary sources. The same procedure was performed for Lake Oeschinen and Lake Thun.

At Lake Thun, the dating of flood layers is not fully independent of the instrumental data. The flood layer sequence was compared with the annual peak discharge at the Hondrich station. Using ^{137}Cs and historic earthquakes (represented as mass-movement deposits and deformation structures in the lake sediments) as independent age horizons, major flood layers could in fact be attributed to the highest annual peak discharges (2005, 1999, 1968, 1944, 1930, 1910).

In the second stage of flood data integration (Figure 2), the flood series dating from 1400 CE onwards were normalized and then smoothed using a 31-yr Gaussian filter to define common flood periods. Principal component analysis (PCA) was performed to explore the variability of the normalized flood data sets over the last 600 years. The first two factors were extracted (rotated and unrotated) from the flood proxies of two floodplains, three lakes, and four documentary flood records. This process was repeated with other combinations of flood series.

The distribution of floods (FA scores) was plotted according to the first factor and then compared to data series of paleoclimate records, including the reconstructed temperature and precipitation curves for the Alps (Dobrovolný et al., 2010; Pfister, 1999) and total solar irradiance (TSI; Steinhilber et al., 2009). Finally, the integrated paleoflood series were associated with the atmospheric variability of PCA scores of the Summer North Atlantic Oscillation (SNAO).

3.6 Atmospheric simulation

Once the flood periods had been defined using the past anomalies of the integrated flood series from the Bernese Alps, paleo-climate simulation of the SLP anomalies was performed from 1400 CE onwards to explore the interannual variability of atmospheric patterns in relation to flood frequency (Figure 2).

First, the atmospheric variability was inferred from the SLP grid taken from the 20th Century V2 Reanalysis Project (20CRP; Compo et al., 2011). The 20CRP is a mission of NOAA/OAR/ESRL PSD (Boulder, Colorado) that produces

reanalyses of weather maps covering the period from 1850 CE onwards with a horizontal spatial resolution of 2°.

According to Peña and Schulte (2014) and Peña et al. (2015), an empirical orthogonal function (EOF) analysis (i.e. PCA) of SLP summer anomalies (July-August) was performed to define the variability of atmospheric modes for a period of observation that extended from 1850 to 2010 CE. July and August were chosen because 95% of historical floods in the study area over the last 500 years occurred during these two summer months. EOFs were determined for the East Atlantic-North Europe domain. Prior to the EOF analysis, each grid point was corrected by the square root of the cosine of the latitude. The corrected grid points were used to compute the covariance matrix. To assess whether the EOFs are clearly separated, the scree-test criterion was used.

The SLP grid used from 1400 to 1849 CE in the present study was provided by the Last Millennium Ensemble Project (LME; Otto-Bliesner et al., 2016) designed by the CESM Paleoclimate Working Group at NCAR. The LME project used a ~2-degree atmosphere and land and a ~1-degree ocean and sea ice version of CESM-CAM5_CN (1.9x2.5_gx1v6). The 13 CESM-LME full-forcing simulations, including solar intensity, volcanic emissions, greenhouse gases, aerosols, land use conditions, and orbital parameters were used for the inter-annual paleo-climate variability from 850 to 2005 CE (Peña and Schulte, this issue).

Quantile-quantile mapping transformation (Amengual et al., 2012) was used to correct the model. The procedure consists of calculating the changes, quantile by quantile, in the cumulative distribution frequency (CDF) of the daily SLP of the LME outputs and the observed data. The statistical adjustment is based on

the relationship between the i^{th} ranked value P_i (projected or future calibrated), O_i (control observed or baseline), S_{ci} (raw control simulated), and S_{fi} (raw future simulated) of the corresponding CDFs.

The EOF component scores from 1400 to 1849 CE were calculated from the component score coefficients matrix from the PCA. Finally, the EOF reconstructed series for the period 1400-2010 CE were plotted alongside the integrated paleoflood series and visual correlations were made to explore climate pattern of atmospheric variability of flooding.

4. Analysis of past floods by archive type

In the sections that follow, the different archive types for the Bernese Alps flood series are presented and discussed. Some of these data series have been previously published and so the discussion adheres, in the main, to the interpretation provided by their authors. Other flood series are unpublished data. Finally, raw data were compiled from data bases and other sources and were re-processed and then interpreted.

4.1 Floodplain geomorphology and sedimentary records

The floodplains of the main Alpine valleys and deltas in Switzerland provide excellent archives for reconstructing a continuous flood history for the last 3200 years (Schulte et al., 2004; 2008; 2015; Laigre et al., 2013). Over the centuries, fluvial erosion, aggradation, channel shift and avulsion, crevasse splay, effects of embankment, and channel correction have generated a characteristic spatial

imprint of valley floor geomorphology and geology. High resolution sedimentary and geochemical proxy data with decadal to intra-decadal sample resolution were obtained from the floodplain deposits of intradistributary and marginal basins and also channel fills in the Hasli-Aare, Lombach and Lütschine basins (Schulte et al., 2008, 2009a, 2015; Carvalho and Schulte, 2013). Textural and TOC percentages were used to define major and minor deposition cycles, showing mostly fining-upward sequences with organic soil formation at the top. These cycles of coarse-grained, fine-grained and organic beds are also logged by the variability in the geochemical proxies. Although some geochemical flood signal types (such as Zr/Ti, Zr/Rb, and Sr/Ti among others) have been used in numerous paleoenvironmental studies (Kylander et al., 2011; Jones et al., 2012), geochemical proxies have to be rigorously investigated and selected afresh from catchment to catchment. Moreover, because the catchment lithology of the Bernese Alps also presents marked differences according to the specific geological and tectonic settings of each basin, chemical elements and ratios were plotted individually alongside texture, TOC, and lithostratigraphy, to determine the most appropriate flood proxies.

For example, peaks of higher Ca/Ti ratios in the floodplain records of the Lütschine delta (from 2600 to 1000 cal yr BP) and in those of the Lombach fan delta (from 2300 to 1200 cal yr BP) were interpreted as flood pulses. These episodes correlate, in the main, to lower solar activity and cooler climate pulses (Schulte et al., 2008, 2009a, 2009b). This pattern is also recorded in the 200-yr old channel fill deposit in the central area of the Lütschine fan delta. Because the sedimentation rates of the delta floodplains have been highly influenced by river embankments and river diversions since the 14th century, the Lütschine

and Lombach flood series are not sufficiently sensitive to provide accurate continuous series for the flood data integration from 1400 CE to present.

Moreover, detailed investigations in the Hasli-Aare floodplain (Schulte et al., 2015) showed that the geochemical imprint of flood layers can vary greatly depending on the provenance of the material transported by the floods. The source of sediment yield in mountain catchments often varies with the spatial distribution of convective precipitation (thunderstorms) and the contribution of glaciers and snow cover to river discharge. Therefore, Principal Component Analysis was performed on the geochemical elements in the core samples. The Factor 1 loadings of the floodplain deposits of the mid-size Hasli-Aare (596 km^2) catchment were defined, on the one hand, by Zr, Sr and Si, that is, the elements associated with the coarse-grained flood sediments eroded from the highest headwater catchment dominated by intrusive rocks; and, on the other, by Mn, Al, K, Ti and Fe, that is, the elements associated with the fine-grained deposits from minor floods, which are related to the erosion of metamorphic rocks and soils of the middle stretch of the Hasli-Aare basin (Schulte et al., 2015).

The lithology of the small 4-km^2 Eistlenbach catchment, however, is different. Sedimentary rocks, including limestone, sandstone, and marls, dominate the higher area of the catchment, while heterogenic Pleistocene moraine deposits are found at lower altitudes. The Factor 1 loadings of the chemical composition of samples were defined, on the one hand, by Zr, Al, Si, Ca and Sr, elements associated with coarse material from the higher catchment, and, on the other hand, by Ti, Fe and Mn, elements associated with fine-grained material from the lower catchment and from eroded soils, and, additionally, by Zn, Pb, and Cu, attributable to the trapping of metals by organic layers and soil horizons.

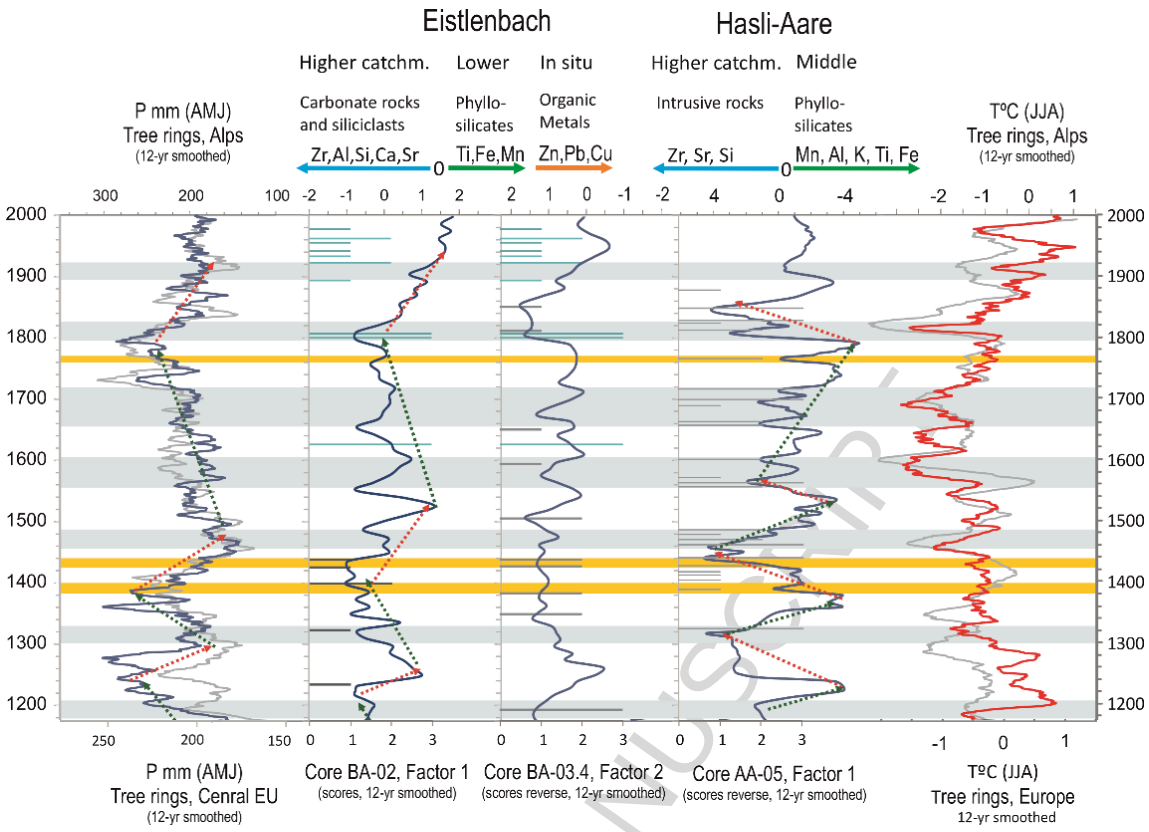

Figure 3: 12-yr smoothed geochemical flood proxies (Factor 1 and 2) from floodplain deposits of the Eistlenbach (Schulte et al., 2016; unpublished data) and Lower Hasli-Aare catchments (Schulte et al., 2015). Cool climate flood pulses shaded blue and warm climate flood pulses shaded yellow. Black bars represent coarse-grained flood layers. Blue bars represent documentary flood magnitudes. Precipitation and temperature reconstruction from tree rings according to Büntgen et al. (2011). Dashed arrows represent trends of geochemical proxies and late spring precipitation. Note the reverse trends between the geochemical flood proxies of the higher and larger Hasli-Aare catchment and the lower and smaller Eistlenbach catchment.

Figure 3 shows the geochemical flood proxies since 1180 cal yr BP as inferred from the key sections of the two catchments. Geochemical anomalies representative of increased flood dynamics (shaded areas) in both catchments are identified for the following periods: around 1200, 1320, 1400, 1450, 1560, 1660, 1760, 1800 and 1910 cal yr CE. Seven of these ten flood periods correspond to cool climate pulses as defined by the paleoclimate tree ring data reconstructed by Büntgen et al. (2011). When low-frequency trends of geochemical flood series are compared with the late spring-early summer

precipitation (AMJ) two different patterns are described because these trends mirror the provenance of the floodplain sediments depending on different erosion processes and flood mechanisms. During humid climate pulses, contributions from the lower and middle Hasli-Aare catchments, with respective mean elevations of 1578 m a.s.l. and 2171 m a.s.l., are noted. Concurrent with this, the floodplain records of the Eistlenbach basin, presenting the highest elevation at around 2204 m a.s.l., show catchment-wide connectivity. During dry climate pulses, the contribution from snow and glacier melt in the highest areas of the Aare catchment (plutonic rocks; mean elevation of 2528 m a.s.l. and highest elevation of 4273 m a.s.l.) increase, whereas the Eistlenbach headwater is disconnected from the distal areas where the aggradation of fine-grained deposits is related mostly to local soil erosion and *in situ* soil formation.

The spectral analyses performed on all floodplain data series, $\delta^{18}O$-records from Greenland ice cores (GISP2; Reimer et al., 2004) and TSI (Steinhilber et al., 2009), show similar periodicities of 200 and 90 years corresponding to the Suess and Gleisberg solar cycles. These teleconnections are, in all likelihood, the result of the dominant influence of solar activity and North Atlantic atmospheric dynamics (Schulte et al., 2008, 2015; Glur et al., 2013).

4.2 Flood records from lakes

In the four lake-sediment sequences studied, layers characterized by their higher density and coarser grain size and composed of autochthonous minerogenic and organic matter were found. Based on these characteristics, the layers were interpreted as having resulted from past flood events (Wirth et al.,

2011, 2013; Glur et al., 2013; Amann et al., 2015). A total of 138 flood layers over the last ca. 1100 years have been identified in the Oeschinen sequence (i.e. a mean of 0.12 floods per year), 86 over the last ca. 9,300 years in the Grimsel sequence (i.e. a mean lower than 0.01 floods per year), 148 over the last ca. 10,000 years in the Iffig sequence (i.e. a mean of 0.015 floods per year) and 18 over the last ca. 150 years in the Thun sequence (i.e. a mean of 0.11 floods per year).

The varying degree of sensitivity of the lake sediments to the recording of floods might be attributable to two causes: one related to the methodological differences in the identification of flood layers at each site; the other related to different catchment sensitivities to flood events as reflected in their different geology and geomorphology. In the first instance, macroscopic observations and measurements (GEOTEK, grain size) allowed mm-scale flood layers to be identified in the sediments of Lake Thun, Iffig, and Grimsel, while sub-mm flood layers could be identified in the Lake Oeschinen sequence using thin section micro-stratigraphy. These methodological differences in flood layer identification could influence the data and, hence, the interpretation of a lake's sensitivity to flood events.

The second explanation for the varying degrees of flood sensitivity encountered can be linked to the amount of easily erodible material in the different catchment areas. By order of erosion potential (from highest to lowest): erodible sandstone and shales make up the northern area of the Lake Oeschinen catchment (Tertiary flysch), while Jurassic and Cretaceous limestones dominate its southern area; Cretaceous limestones make up most of the Lake Iffig catchment, while barely erodible granite and granodiorite characterize the Lake

Grimsel catchment. Lake Thun integrates all the above lithologies. However, here sedimentary rocks are particularly dominant, since, upstream, Lake Brienz acts as a sedimentary sink for a large part of the catchment dominated by crystalline rocks.

Glaciers are also a significant erosion factor, greatly increasing the availability of erodible material, regardless of the catchment geology. For instance, the glaciers of the Oeschinen catchment (Blüemlisalp Glacier) have supplied a significant amount of glacial material over recent millennia that is readily eroded today, i.e. even when flooding is only moderate. Conversely, the absence of significant glacier coverage eroding the hard crystalline rocks of the Grimsel catchment may limit the availability of material for erosion when a flood occurs (the situation that prevailed before the damming of the hydropower reservoir in 1932 CE, which incorporated the old Grimsel Lake (see section 2)). Thus, only high-magnitude flood events may have sufficient energy to erode the few materials available. This might explain the very few flood events recorded in the Grimsel sequence, whose background sediments are otherwise dominated by organic-rich sediments.

The flood variability recorded in the paleoflood series of the Iffig, Grimsel, Oeschinen, and Thun Lakes requires that we account for i) the different hydro-meteorological processes that produced flooding in either the small mountain streams (Iffig, Grimsel and Oeschinen) or the large river (Thun), but also for ii) the different intrinsic properties of the records, such as their varying degrees of sensitivity. Glur et al. (2013) and Wirth et al. (2013) circumvented these issues by i) calculating flood frequencies in percentages, as opposed to floods per year, as this gives a common range of variation and ii) stacking all these flood

frequencies to obtain a regional picture of flood variability, independent of differences, for example, in hydro-meteorological processes.

To compare the flood records of the four lakes and to account for any variability in the hydro-meteorological processes across the sites, the issue of different sensitivities has to be addressed and rectified. Buffering the different lake sensitivities requires a similar number of events per lake, retaining only the high-magnitude events recorded in all the records. However, applying such a filter requires knowing the magnitude of each flood event in each series. Previous studies have shown that flood magnitude can be reliably reconstructed from either the flood-layer thickness, the total deposited flood-sediment volume or the grain size (see Wilhelm et al., 2018 for a review). Since only flood-layer thickness is known for the Iffig, Grimsel and Oeschinen paleoflood series (Figure 4), this characteristic was deemed to be a relevant flood-magnitude proxy and, thus, used when applying a threshold to obtain a similar number of events for all records. Given the very few flood layers recorded in the Grimsel sequence, a 9.5-mm thick threshold was applied to the Oeschinen record (48 layers identified over the last 1000 years) to obtain a number of events similar to that for the Iffig record (44 layers over the same time period).

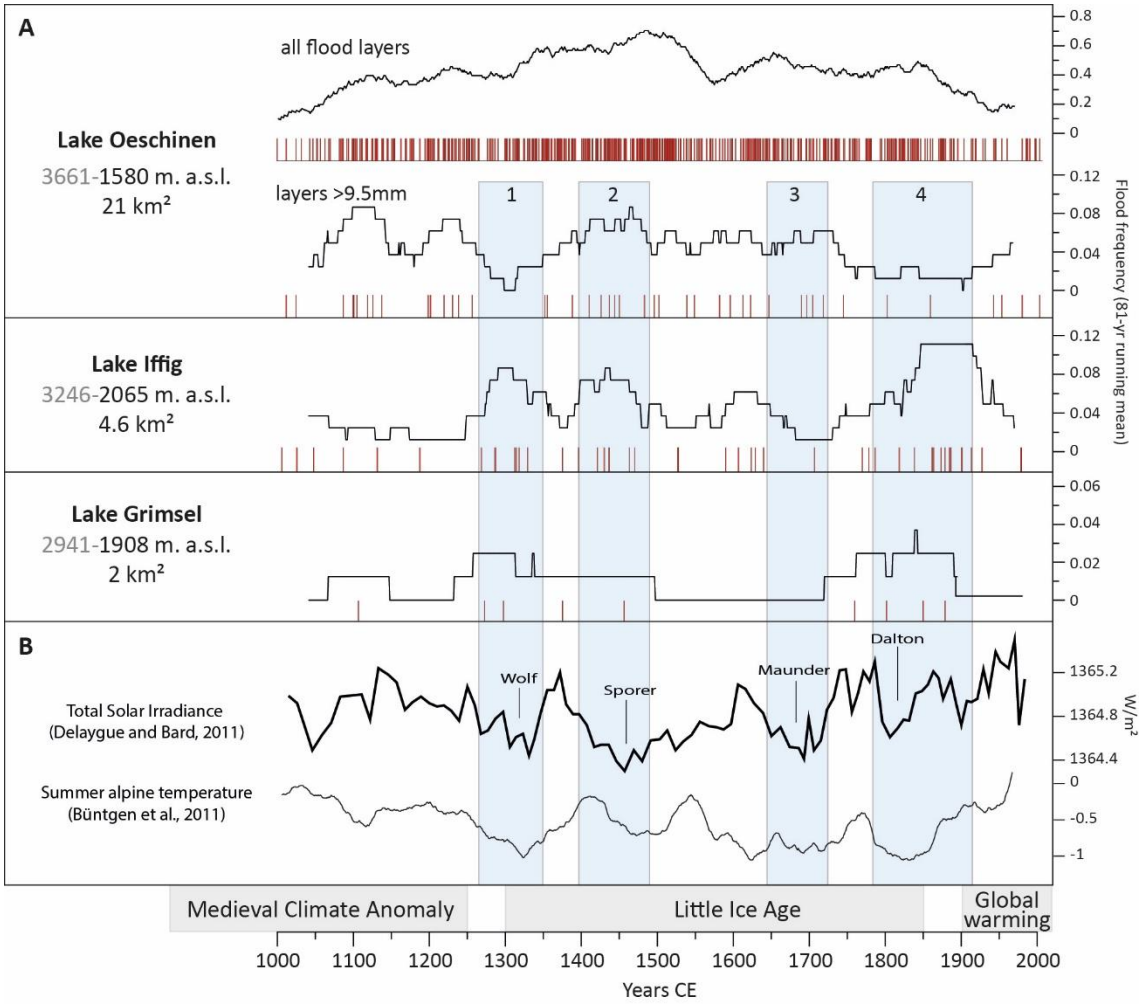

Figure 4. (A) Comparison of flood frequency based on lake records in the Bernese Alps. Red vertical bars represent the flood layers identified in sediment sequences of Lakes Oeschinen, Iffig and Grimsel over the common period of the last millennium. Curves represent the variability in flood frequency smoothed using an 81-yr running mean of flood layer occurrences. Shaded blue bars highlight the specific periods discussed in the text. (B) Total solar irradiance (Delaygue and Bard, 2011) and summer alpine temperature (Büntgen et al., 2011) are shown to illustrate possible linkages with the reconstructed flood frequencies.

The lake paleoflood series depict a highly variable flood frequency over the last millennium, which is the common period covered by the Oeschinen, Iffig and Grimsel records (Figure 4 A). The main feature of the Oeschinen record are the two flood-poor periods of 1270-1350 and 1800-1900 CE, while the Iffig and Grimsel records are characterized primarily by the flood-rich periods of 1250-

1350 and 1750-1950 CE (periods 1 and 4, Figure 4A) in concordance with the sedimentary floodplain records from the Hasli-Aare (Schulte et al., 2015) and, furthermore, in the case of the 19th century, with the documentary flood records for the main valleys presented in section 4.3.

These periods correspond, respectively, to climate transitions from the Medieval Climate Anomaly (950-1250 CE) to the Little Ice Age (1300-1850 CE) and from the Little Ice Age to Global Warming. The variable behavior illustrated by the records cannot be explained by differences in hydroclimate since all the sites are located in the same area. A better explanation might be afforded by the variation in the response of the geomorphic system to precipitation events and to their spatial variability. The Lake Iffig and Grimsel records present similar features of flood frequency and both originate from catchments of very similar characteristics (size, elevation, and land cover). Compared to these catchments, the Oeschinen catchment is characterized by a lower lake elevation (1580 m a.s.l.), a larger surface area (21 km^2), a higher catchment elevation (3661 m a.s.l.), and by the presence of significant glaciers (30% of catchment). While localized convective events such as thunderstorms (resulting in strong rainfall intensity over a restricted area) might affect the small-scale catchments of Lakes Iffig, Grimsel and Oeschinen in a non-homogeneous manner, larger precipitating systems associated with large-scale atmospheric situations might affect these catchments more evenly, as occurred during the 1831 and 2005 CE events (Wirth et al., 2013; Amann et al., 2015). However, we should not overlook the well-documented large scale event of 1762 CE, when precipitation primarily affected the eastern basins (Hasli-Aare). This pattern is accurately reflected by a thick flood layer in the Lake Grimsel record and the

lack of significant flood layers in the Iffig and Oeschinen Lake records (Figure 12).

If we consider all the Lake Oeschinen flood layers (no threshold applied; Figure 4A), the period 1800-1890 CE emerges as one of the richest on record with frequent flood deposits. This suggests that during the 19th century the Lake Oeschinen record was sensitive to a high number of hydro-meteorological events of both types, i.e. large-scale atmospheric systems and localized convective events. During this same period, documentary sources record five severe rainfall and three severe thunderstorm events (Figure 5).

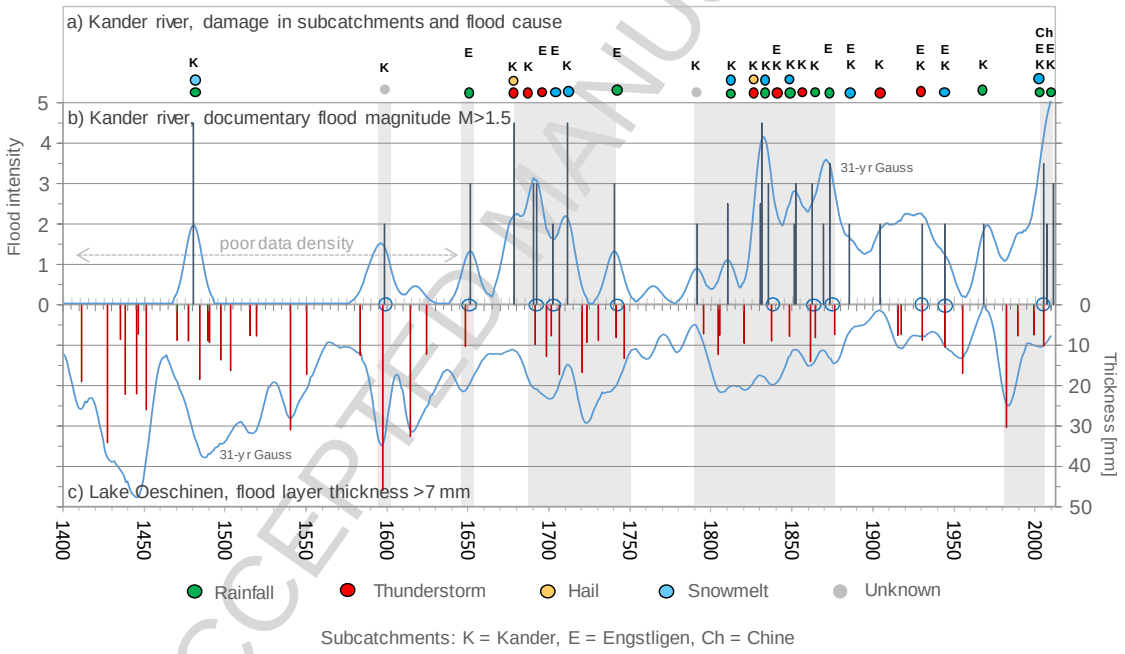

Figure 5. Comparison of flood events and their causes as documented in the historical sources for the Kander catchment (b) (this study) with floods recorded in the Lake Oeschinen record (c) (Amann et al., 2015). A 7-mm thickness threshold was applied to the latter record to obtain a similar number of events (28) as that of historical flood events (26) since 1640 when the documentary flood event density is homogeneous. Flood data series smoothed with a 31-yr Gaussian filter. Cause of flood events (a) shown by coloured dots. Capital letters represent the affected sub-catchments of the Kander valley.

According to Amann et al. (2015), who conducted meteorological reanalyses at the flood dates recorded in Kandersteg, the flooding of the lower (558 m. a.s.l.) and larger (1126 km^2) Kander valley is strongly linked to large-scale atmospheric processes. A comparison of the Lake Oeschinen record and the historical flood events recorded in the Kander River (this study) supports this hypothesis. When comparing the occurrence of Kander flooding with Oeschinen flood events between 1640 and 2010 CE (Figure 5), after applying a 7-mm thickness threshold to obtain a similar number of events, 11 lacustrine events were found to be synchronous (blue circles) with 24 historical events of magnitude M>1.5, within dating uncertainties of the lake record. Moreover, the flood frequency of the historical events mirrors that of the lacustrine record, both of which highlight flood-rich periods in ca. 1680-1750, 1790-1880, 1920-1950 and 1999-2008 and flood-poor periods in ca. 1620-1680, 1750-1790, 1880-1900. This clearly suggests that approximately half the broad-scale, high-magnitude floods recorded in the Kander River also occurred in Lake Oeschinen and, hence, that there is a link here to large-scale atmospheric processes.

Previous compilation studies aimed at providing a regional overview of paleoflood variability in the Alps have reported a regional link to temperature (Glur et al., 2013; Wirth et al., 2013). These studies identified more frequent floods during cold periods that might be linked to low solar activity and to changes in North Atlantic circulation. Similar findings are also observed when comparing the individual records from Lakes Iffig and Grimsel (this study) to summer alpine temperature and total solar irradiance (periods 1, 2, 3 and 4; Figure 4 B). The correspondence between solar minima, cold temperatures and

higher flood frequency is clearer in the Lake Iffig record (periods 1, 2, and 4) owing to the higher number of flood events. The asynchronicity of ca. 70 years in the case of period 3 may be related to the range of ^{14}C dating uncertainties. When considering all the flood layers in the Lake Oeschinen record, Amann et al. (2015) also reported more frequent floods during the colder and wetter periods of the last millennium. When applying the filter (9.5-mm thickness threshold), flood variability describes a diametrically opposite pattern during the two climate transition periods (periods 1 and 4; Figure 4). This might be pointing to changes in the dominant hydro-meteorological processes.

4.3 Historical flood series

The "visual correlation" between the four historical, documentary evidence-based flood series (a: Hasli-Aare, b: Lütschine, c: Kander and d: Simme Rivers) is surprisingly good (see blue shaded periods in Fig.5), taking into account the fact that different catchments, even though they are geographically close, may present significantly different flood behaviors and that data gaps in their respective series can disturb the overall picture. Additionally, it should be stressed that the historical documentary data are not equally distributed over the catchment areas under study here. Graphs 5e (i.e. the integrated historical flood frequency of the Hasli-Aare, Lütschine and Kander Rivers) and 5f (i.e. the flood frequency of the Aare River between Thun and Bern), however, also present a very strong correlation, which, on the one hand, is unsurprising given that these rivers are either direct or indirect tributaries of the River Aare between Thun and Bern, yet, on the other, it should be borne in mind that Lakes

Thun and Brienz have the potential to significantly upset this correlation, especially in the case of smaller flood events due to their respective retention capacities.

Moreover, major (river) engineering interventions, including, for example, the redirection of the River Kander to Lake Thun in 1714 and the construction of hydro-electric dams throughout the nearby catchment (i.e. the catchment basin of the aformentioned rivers) significantly altered the overall hydrological system. Taking all these “disturbances” into account, the correlations may even be considered as being quite exceptional, which points to the generally good reliability of historical documentary flood evidence. According to Figures 6 and 9, the periods of greatest flood frequency occurred between 1820 and 1870 and after 1977, although it should be borne in mind that the density and quality of information varies over time. The increase in flood frequency since 1973 is also a result of the systematic tracking of flood events initiated in that year by the WSL databank. The largest flood event recorded in the catchment as a whole (but not including that of the Simme) is the catastrophic event of 1831, the magnitude of which forced local people to emigrate abroad or to migrate, as has been documented for the village of Matten (Schulte et al., 2009a). Almost as severe as the 1831 event are the flood episodes of 1480, 1851, and 2005 CE.

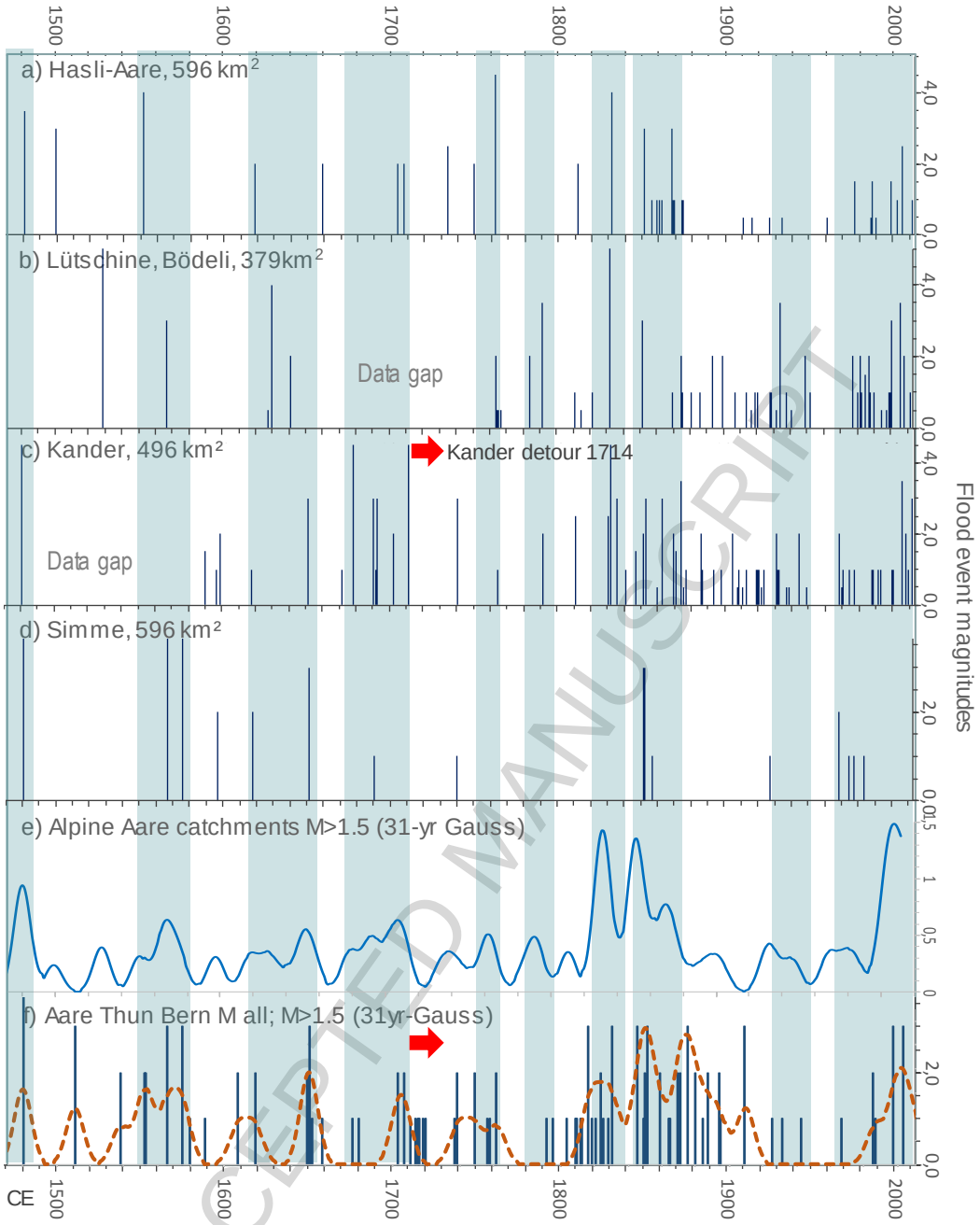

Figure 6: Historical flood damage in the catchments of the Bernese Alps. A) Hasli-Aare River (Schulte et al., 2015), b) Lütschine River (Schulte, unpublished data), c) Kander River (this paper, modified after Bütschi, 2008, and WSL data), d) Simme River (Bütschi, 2008), e) Integrated record of Alpine Aare catchments M>1.5 (31-yr Gauss), and f) Aare River from Thun-Bern (Wetter, data collection; all magnitudes and M>1.5, 31-yr Gauss). Flood-rich periods are indicated by blue shading. Bars in figures represent the magnitude of flood damage. Curves in panels e) and f) represent 31-yr Gauss smoothed flood frequency of the alpine catchments and the Aare River from Thun to Bern.

Figures 6e and 6f (periods shaded blue) also reveal differences, for example, the 1511 flood which, according to documentary sources, was an extreme event that involved the major rivers of the Aare, Rhine, Limmat, and Reuss. This event is missing in the tributaries of the alpine Aare catchments upstream of Lake Thun, except that of Hasli-Aare. Various explanations are plausible. Either the region of interest (i.e. that formed by the tributaries) was, indeed, not greatly affected by flooding or the event simply went unrecorded for reasons that remain unknown. In 1762, a flood event presenting a similar pattern also appears to have occurred. In this case, the Lütschine (Fig. 5b) and Kander (Fig. 5c) catchments have no record of flooding, whereas the Hasli-Aare valley (Fig. 5a) is reported as having suffered one of the most catastrophic floods of the last 500 years, responsible for major changes to the river floodplain and channel morphology (Schulte et al., 2015). According to Röthlisberger's (1991) flood data compilation, most of the river catchments on the northern flank of the Alps to the east of the Hasli valley were affected by catastrophic floods. This suggests that the differences between the western and eastern catchments of the Bernese Alps resulted from the easterly locations of the precipitation field.

In addition, the lack of correspondence between Figures 6f and 6e – specifically, the flood gap in the River Aare between Thun and Bern between the late 1760's and the early 1790's – might be the result of the redirecting of the River Kander into Lake Thun. This means that its retention capacity downgraded the smaller River Kander – as it was in that period – and the River Lütschine's flood events to such an extent that contemporary observers, downstream of Lake Thun, no longer considered them worthy of being recorded. Likewise, the lack of correspondence between the two figures (6f and

6e) between the late 1920s and late 1980s can be attributed to the same reason, except that the floods of the tributaries were probably not so effectively downgraded given what eventually would have been the lower retention capacities of Lake Brienz and Thun. This could have been triggered by different meteorological situations (e.g. longer lasting melting of ice and/or periods of rain resulting in significantly fuller lakes) to those that prevailed in the earlier period. Alternatively, the lower retention capacities might have been caused (arguably more plausibly) by the flood mitigation constructions on the Hasli-Aare (levees and river correction since 1876) and Lütschine Rivers (levees since the 1870s) and the straightening, in parts, of the River Kander which, due to increased runoff and the removal of flood retention along the river banks, may have filled the lakes with significantly more water and reduced, in like manner, their retention capacities. A further explanation for the apparently higher number of small flood events (compared to the period 1760-1790) downstream of Lake Thun might be that observer perceptions of these events changed, perhaps because of an increased risk awareness given the value of infrastructure under threat.

4.4 Instrumental flood discharges and calibration

Flood frequencies and magnitudes reconstructed from natural and documentary archives can be calibrated using instrumental data series. However, in mountain river catchments these reference periods are usually short when compared to those of the cities of the Alpine foreland and lowlands (e.g. Basel, Vienna, Prague or Cologne). In the Bernese Alps, the discharges of the Hasli-Aare and

Kander Rivers and those of the Lütschine River have been measured systematically since 1903 and 1908, respectively.

Schulte et al. (2015) have attributed the Hasli-Aare River peak discharge measurements to flood event intensities, which are classified according to the damage reported in textual sources and to changes in the floodplain morphology. The flood magnitude M=1 threshold is attributed to discharges recorded at the Brienzwiler gauge station of between 360 m^3s^{-1} and 370 m^3s^{-1}. Above these values, the river starts to overtop the embankments, which were constructed in 1875 to protect the 1-km wide floodplain of the lower Hasli valley. The average to severe sized flood threshold is defined by flood magnitude M=2 and corresponds to a peak discharge of 420 m^3s^{-1}, while catastrophic floods have an estimated discharge of around 500 m^3s^{-1} (M=3.5). Before the Aare River correction in 1875, this highest threshold was reached in 1480, 1551, 1762 and 1831 CE.

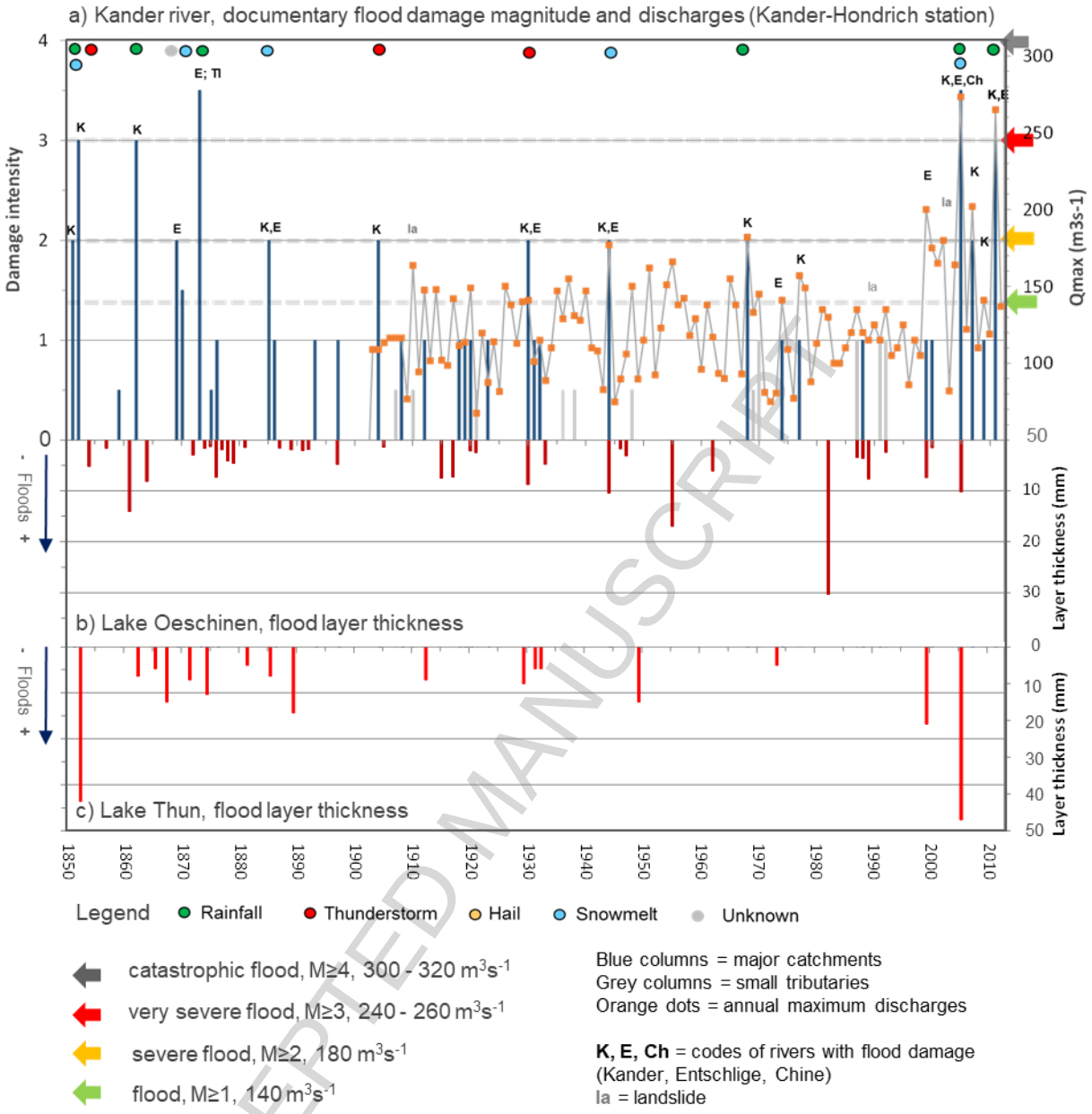

Figure 7: Top: annual peak discharges and documentary evidence-based flood frequencies of the Kander River since 1850 CE. Blue bars represent flood damage intensities and orange dots are peak discharges. Arrows represent thresholds of flood magnitude classes. Bottom: flood frequencies reconstructed from flood layers of Lake Oeschinen (center) and Lake Thun (>5mm; bottom). Red bars show flood layer thickness.

However, since 1932 CE, floods have been mitigated by the retention capacities of several interconnected reservoirs built to generate hydroelectric power. In particular, this has affected spring and early summer floods because of the fall

in reservoir levels after a period of maximum electricity production during the cold winter months. Under the present river configuration, the 2005 CE event recorded a peak discharge of 444 m^3s^{-1}, corresponding to a magnitude of M=2.5, but, without this enhanced reservoir retention capacity, it could have reached an intensity of 563 m^3s^{-1} (M=4.5), according to calculations made by the power company Kraftwerke Oberhasli AG.

Unlike the Hasli-Aare River, the Kander catchment is not influenced by reservoirs, and river correction and embankment work are not so well developed. Here, event intensities and thresholds were calibrated using instrumental data that first became available in 1905 at the Kander-Hondrich gauging station. Discharges were attributed to event intensities by interpolation between two anchor points: the discharges of the floods causing the greatest documented damage, i.e. those with magnitudes of M=3.5 and M=3 (recorded in 2005 and 2012, respectively) and the discharges of the average intensity floods (M=2) of 1945, 1968 and 2007. According to this scale, the threshold of the average flood corresponds to 180 m^3s^{-1} while that of the severe flood corresponds to 245 m^3s^{-1} (M=3). The threshold of catastrophic floods was linearly extrapolated to 310 m^3s^{-1}. Minor flood damage in the Kander catchment occurred at discharges of around 140 m^3s^{-1} (Fig. 6).

If we restrict our focus to the reference period and consider solely the contribution of the Kander sub-catchments, the following observations can be made: the flood impact in at least two of three sub-catchments (that is, Kander, Entschlige, and Chine) reached an intensity of M>3 according to flood damage records (Figure 7) and discharge values of >260 m^3s^{-1} were recorded at the Kander-Hondrich gauge station. In the case of the average floods (M=2;

Q>180), different locations were affected: i) during some events, flood damage occurred in one or two sub-catchments and the discharge values recorded at the Kander-Hondrich station were relatively high (1944: 177 m^3s^{-1}; 1986: 182 m^3s^{-1}; 2007: 202 m^3s^{-1}); ii) during other events, flood damage (and higher peak discharges) occurred in just one of the three sub-catchments and discharge measurements at the Kander-Hondrich station (for all sub-catchments combined) were relatively small (1904: 120 m^3s^{-1}); and iii) some floods reached moderate peak discharges (around 180 m^3s^{-1}) in more than one sub-catchment, contributing to moderate-high Q max at the Kander-Hondrich gauging station, although no major damage was reported (e.g. 1999, 2000, and 2002). These different patterns indicate possible uncertainties in the precision and calibration of the documentary and instrumental records.

When comparing flood layer thicknesses and frequencies at Lake Oeschinen (Amann et al., 2015) and Lake Thun (Wirth et al., 2011; Figures 7b and 7c) with instrumental and documentary data, two aspects need careful consideration: i) the uncertainties in the chronological model of the sedimentary record, as defined using different dating techniques, and ii) the factors that control flood layer deposition. As regards the first point, it should be noted that the varved Lake Oeschinen record presents several flood layers that coincide in terms of timing with the Kander floods, as documented by textual sources and instrumental data, but that other flood layers do not correspond at all with the Kander floods. Indeed, sensitivity to local advective and convective rainfall events in the 21-km^2 catchment of Lake Oeschinen can differ greatly as regards the peak discharge recorded at the Kander-Hondrich gauge station, which provides measurements for three sub-catchments with a total area of 596 km^2.

As regards the second point, the flood events from 1850 to 1897 CE systematically show time lags of approximately three years between the historically documented Kander floods and the Lake Oeschinen flood layers. For example, the cluster of Lake Oeschinen flood layers dated between 1869 and 1879 CE may correspond to the Kander flood damage period of 1872 to 1881 CE. This lag is acceptable as it lies within the uncertainty range of varve counting chronologies. However, the thickest flood layer at Lake Oeschinen, dated to 1982 CE, does not coincide with either the Kander floods or with the Lake Thun flood layers. This can be attributed to snow and glacier (30% catchment cover) melt and/or the influence of local thunderstorms on small, high-altitude catchments. In 1982 CE, Central Europe recorded positive summer temperature anomalies of +1.04 ºC (Dobrovolný et al., 2010).

Sediment core THU07-2 in Lake Thun (Wirth et al., 2011) shows some minor flood time lags. In this core, note that the chronostratigraphy is not based on varve counting, but on ^{137}Cs dating and correlation with historical flood data and earthquakes. The thickness of Lake Thun flood layers (filtered by a >5 mm-threshold) shows a good correspondence with the magnitudes of Kander floods. This is due to the fact that the Kander river mouth (despite the possible modification by the Simme River that flows into the Kander River a few km upstream) dominates the sedimentation processes in the western Lake Thun basin. Both flood series, the documentary Kander flood data and the Lake Thun flood layers, are controlled by fluvial processes of the same river system.

Finally, it should be noted that in the Hasli-Aare and Kander catchments, the low to moderate flood magnitudes recorded throughout almost all the 20th century in the documentary evidence are reflected also in the gauging station

measurements. Moderate annual peak discharges have been obtained since records were first kept in 1903 CE, but maximum annual discharges increased after 1977 CE in the Hasli-Aare and after 1999 CE in the Kander Rivers (Figure 7). This pattern is also presented by the floods recorded in Lake Thun, and less clearly so in Lake Oeschinen. Nevertheless, the high discharge values observed since the end of the 20th century, particularly those of the 2005 flood, are not unprecedented, as the documentary flood damage series demonstrate. For example, all flood archives present increased flood frequencies and high magnitudes during the second half of the 19th century.

4.5 Lichenometry and other flood archives

In the Hasli-Aare, Lütschine and Eistlenbach catchments, the Fluvalps Research Group has developed various flood proxies inferred from lichenometry, tree rings and historical buildings. These unpublished data are not presented in the present paper; however, on occasions, we do use the lichenometric data to complete the spatial coverage of the paleoflood event maps in section 7. Therefore, a brief description of these results are provided here.

According to the lichenometric dating obtained along four sections in the higher Hasli-Aare gorges, where the river cuts into plutonic bedrock (Fig. 7), the number of reconstructed flood levels ranges from five to eight in each section. Eight floods between 1998 and 1831 CE were reconstructed in at least two sections, five floods in three sections and two in all four sections. The following documentary recorded floods were dated by lichens: 1762, 1831, 1851, 1910,

1922, 1948, 1960, 1977 and 1998 CE. After the construction of the hydroelectric dams in 1933 and 1950 CE, flood events ceased in the headwater catchment of the Hasli-Aare River (Schulte et al., 2015). Figure 8 shows that after the construction of the Grimsel dam in 1932 CE, the flood peak level decreased from 3.42 m in 1922 CE to 2.00 m in 1948 CE. After the construction of the second dam at Räterichbodensee in 1850 CE, floods have never exceeded the height of 0.80 m attained in 1977 CE. The flood levels before the construction of the reservoirs are currently used to perform hydraulic modeling of paleodischarges (results not shown here).

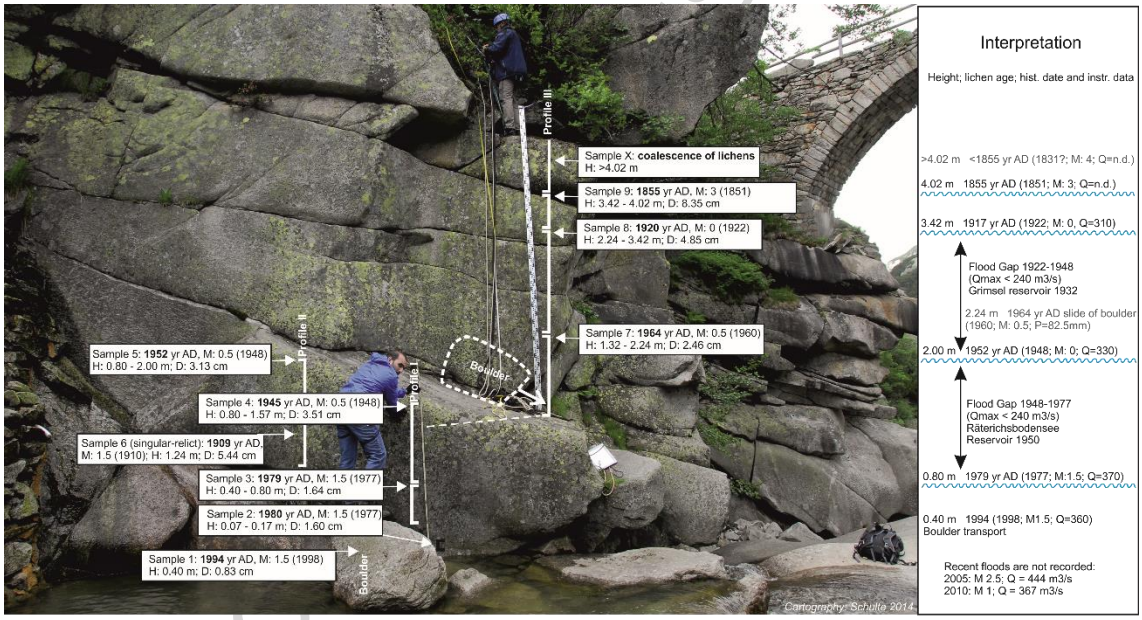

Legend:
Sample 1:
1997 yr AD = Age year AD reconstructed from lichenometry
H: 0.40 m = Height
D: 0.83 cm = Lichen size
M: 1.5 (1998) = Reconstructed flood magnitud and year from historical sources
Q: 360 m3/s = Qmax referes to Gsteigwiler gauging station (river mouth of Aare)

Figure 8: Photograph of the lichenometry profile HA-1 at the Large Begelli bridge in the Higher Hasli-Aare Valley. The gorge's rock surfaces were colonized by lichens after the impact of the Aare River floods. Flood level heights can be dated by measuring the lichen thali of *Rhizocarpon macrosporum* and *Rhizocarpon geographicum ssp. frigidum.*

5 Integration of multi-archive datasets

This section outlines the process of selection of the flood data series discussed separately by flood archive type in the subsections above and describes the process of integration of the flood series selected in a master curve extending from 1400 to present. This time interval was chosen because the documentary flood data are available from the 15th century onwards. Finally, the integrated paleoflood series are compared with paleoclimate time series and atmospheric forcing is investigated (section 6).

5.1 Selection of flood series for integration

To integrate the flood archive proxies, the flood series must fulfil the following criteria: i) cover at least the last 500 years; ii) provide a continuous record; iii) show similar sample density after filtering; and iv) not be affected by major disturbances. Thus, the Lake Thun flood layer record, the lichenometric dating of flood levels, and the instrumental data were not considered for integration because these series are too short (criterion i). The historical flood records of the Alpine Aare catchments were integrated into one single data series (AlpHIST), while the pre-alpine Aare Thun-Bern data (TuBeHIST) were not integrated and were used as a single file for further statistical processing. The flood series since 1400 CE (M>1.5) were normalized and then smoothed with an 81-yr Gaussian filter (the Gleissberg solar cycle frequency) to investigate common flood periods.

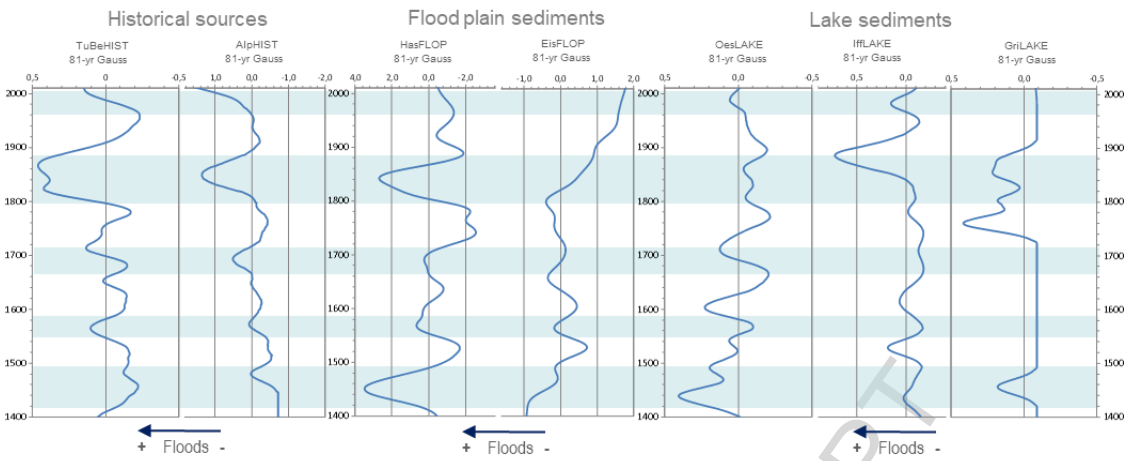

Figure 9. 600-yr long flood series (81-yr Gauss smoothed) of the Bernese Alps according to archive types CE 1400-2010. Flood periods are shaded.

Figure 9 presents seven normalized and filtered flood series with five periods of enhanced flood frequency from 1420-1490, 1550-1590, 1660-1710, 1810-1880, and 1970-2010 CE (areas shaded blue). The historical flood series (TuBeHIST and AlpHIST; M>1.5) and the Hasli-Aare floodplain record (HasFLOP) present a close correspondence from 1480 CE onwards. This correspondence is also partially visible when these pulses are compared with the geochemical flood evidence of the marginal Eistlenbach floodplain (EisFLOP). After 1820 CE, however, any correspondence ceases because the Eistlenbach sediments present a lower variability, probably a consequence of embankments, bed load barriers and land use.

The lake records (Figure 9; frequencies of floodlayer thickness smoothed by an 81-yr Gauss filter) show different patterns to those of the historical flood series and the floodplain records described above. The three lake records coincide during the flood periods of around 1450 and 1870 and after 1977 CE (with the exception of Lake Grimsel, which was affected by the building of the Grimsel reservoir lake in 1932, so that post-1932 it provides no more flood records),

corresponding also with the historical and floodplain records for these periods. As discussed in section 4.2, divergences in the series may have multiple causes: different data densities and influence of applied thresholds; uncertainties of the radiocarbon age model for Lakes Iffig and Grimsel; different physiographic settings (catchment area, altitude, slopes, orientation, and glaciated area) and resultant sensitivity of records to erosion processes; and the regional distribution of precipitation.

Finally, it should be noted that the deviation in the flood records in some specific points may also be attributable to local physical factors and anomalies. For example, the severest event of 1762 CE in the Hasli-Aare floodplain is well documented in the sedimentary sequence of core AA-05, but only a weak signal was obtained for core AA-10 because this site was flooded by the rising lake level of Lake Brienz (documentary data), which influenced its texture and geochemistry.

5.2 Integration of flood series

Factor analysis (FA) was computed to test the variability of the normalized flood data sets over the last 600 years and to generate an integrated flood curve for the Bernese Alps. The first two factors were extracted (rotated and unrotated) from the flood proxies of two floodplains, three lakes, and four documentary flood records. This process was repeated but excluding the Lake Grimsel and Lake Iffig series, because of their low temporal sample resolution and because of the possible 70-yr lag of the flood pulse around 1600 CE (section 4.2), which could be a climatic signal or an effect of the radiocarbon age-model uncertainty.

In the case of the third setting, the four Alpine documentary flood series were integrated into one single series. The FA was then applied to the flood series AlpHIST, Th-BeHIST, HasFLOP, and OesLAKE.

The 2-D plot of the first two factors shows a similar distribution for the three settings. The first factor (40% of the variability in setting three) is defined by the positive loadings of Lake Oeschinen and the negative loadings of the Hasli-Aare floodplain and the historical Aare flood series. Thus, on the one hand, Factor 1 explains the difference between the flood records located in the lower main valleys and those located in the higher lakes in smaller catchments. Factor 1 may also mirror the differences in the frequency of events in these two very different environments. On the broad valley bottom of the lower main valleys, floods are only recorded when the core site, and infrastructure or villages, which are located at some distance from the main channel, are reached by rising water levels and affected by the flow. However, because the river channels are often confined by levees or embankments, the event frequency is relative low. This contrasts with the Lake Oeschinen catchment, which is characterized by steep slopes of what are, in part, highly erodible materials. Given the large number of flood layers and their correlation with the monthly mean precipitation (Amann et al., 2015), it seems that Lake Oeschinen records not only major floods but also the erosion processes of the smaller events and, furthermore, sediment yield from glaciers (30% catchment surface).

The distribution of floods (FA scores) was plotted in accordance with Factor 1. Negative scores represent floods, whereas positive scores indicate discrete or no flooding. The composite flood series of the Bernese Alps presents six quasi-cyclic flood pulses from 1400 to 1840 CE (mean recurrence around 75 years).

The severest flood period with three maxima occurred from 1840 to 1890 CE, whereas the period from 1890 to 1977 CE is defined by a flood gap. In addition to climate factors, this flood gap has clearly been influenced by the implementation of structural flood mitigation measures, including levees, canals, and reservoirs, since the end of the 19th century. Flooding returned from 1980 CE onwards, reaching flood intensities (negative scores) that are nearly as high as those reached during the 19th century.

5.3 Comparison of the integrated flood series with paleoclimate reconstruction data

Figure 10 compares the composite flood series for the Bernese Alps (flood pulses identified shaded blue), the reconstructed variability of the 31-yr Gaussian filtered annual and seasonal temperatures of Central Europe (Dobrovolný et al., 2010), and the precipitation levels in Switzerland (Pfister, 1999) from 1500 to 2010 CE. It can be seen that the flood pulses are related to different precipitation and temperature trends as well as to various combinations of the two.

The flood pulses from 1550 to 1900 CE occurred during negative annual and summer precipitation anomalies. From 1650 to 1995 CE, the winter precipitation series corresponds most closely with the integrated flood series. However, Lakes Ifffig, Grimsel and Oeschinen cannot directly reflect this winter signal as they are frozen during winter and flooding of the main rivers does not occur during winter months either. We believe that during the Little Ice Age the winter signal (high snowfall) might have been transferred to the summer season, influenced also by a delay in the melting of snow cover and glaciers.

Dry autumns coincide with floods from 1700 to 1880 CE, whereas spring precipitations show a random pattern.

When flood pulses are matched to temperatures, a rather heterogeneous picture emerges. Four flood pulses (one around 1760 CE and three between 1810 and 1880 CE) occurred during cold annual and seasonal (winter, spring, summer, and autumn) temperatures. Furthermore, the flood period around 1560 CE coincides with a decreasing temperature trend. The flood cluster around 1700 CE followed on from the coldest (annual and seasonal) climate pulse – the solar Maunder Minimum – with a time lag of less than 10 years. The seasonal temperatures during the 1650 CE flood period show no clear anomalies nor trends, whereas the floods since 1990 CE have occurred during the warmest climate pulse of the last 500 years.

A dry climate may reduce snow cover, but it might also contribute – in combination with the warmer temperatures during summer months, which are synchronous with the seasonal flood period – to increased snow and glacier melt.

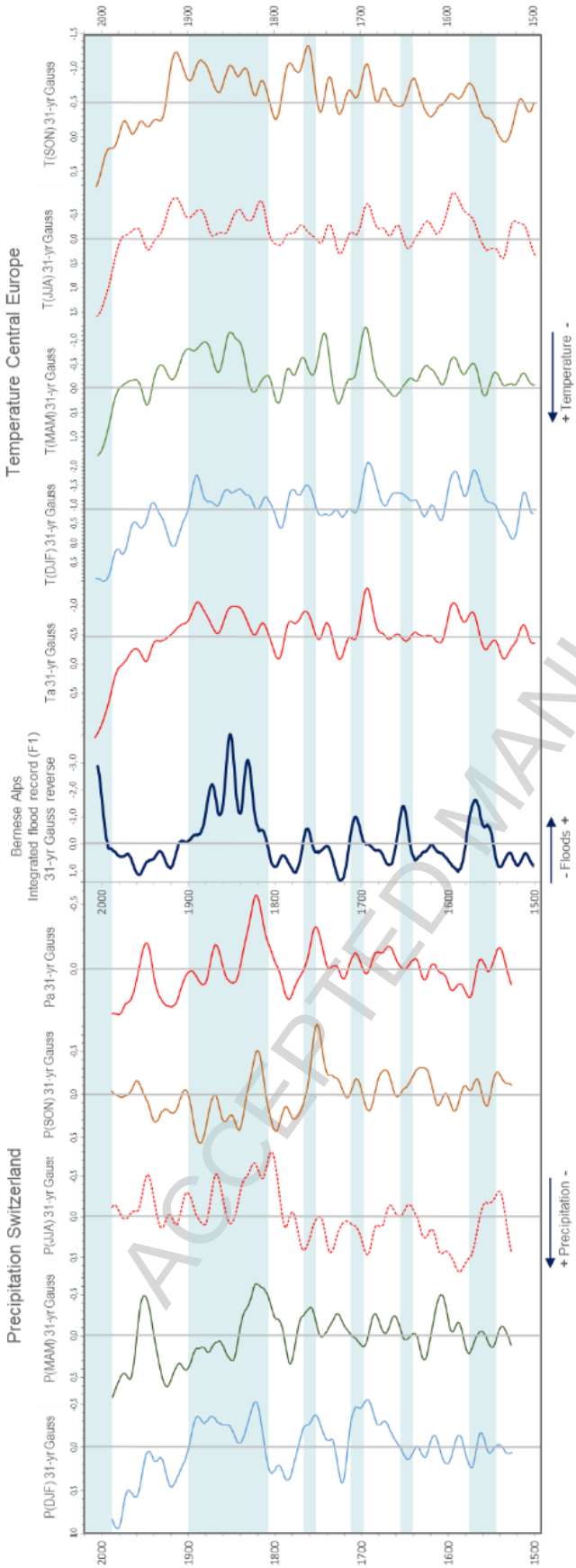

Figure 10. Integrated flood record of the Bernese Alps (dark blue curve in the central section) from 1500 CE to the present, compared to seasonal precipitation of Switzerland (curves to the left; Pfister, 1999) and seasonal temperature of Central Europe (curves to the right; Dobrovolný et al., 2010) reconstructed from historical and instrumental data series. All series are normalized and 31-yr Gauss smoothed.

However, the coincidence of floods with the cooler climate of the Little Ice Age may indicate the relevance of greater water storage due to larger glaciers and more extensive snow cover susceptible to melting processes (Schulte et al., 2015). This in turn produces higher base discharges and surface runoff during summer months (Stucki et al., 2012). Moreover, the permanence of snow cover during summer months promotes surface runoff on slopes during the summer flood season. Rainfall episodes combined with lower soil permeability due to frozen or water-saturated soils, snow cover and snow patches can contribute substantially to flooding in mountain topographies.

In contrast, these factors may interact differently during warm climate periods, such as the one experienced at the end of the 20th century. Remote sensing exercises (Cabrera et al., 2016), which measured the area of snow cover in the Hasli-Aare catchment using satellite images before and after the flood events from 1986 to 2012 CE, recently revealed that snow cover during the years of the severest floods (1987 and 2005 CE) occupied the smallest area. This leads us to hypothesize that, during the warmer climate pulses, a combination of intensive or long-lasting liquid precipitation, a high snow line, and less snow cover involve a greater proportion of the Hasli-Aare catchment in terms of runoff processes.

Finally, one of the most relevant factors for flooding is the intensity and duration of precipitation, which are controlled by atmospheric processes and variability.

Earlier paleoflood studies conducted in the Hasli-Aare catchment (Schulte et al., 2015) indicated possible relations between sedimentary floodplain proxies and the North Atlantic Oscillation (NAO) between 1667 and 1820 CE and the Summer North Atlantic Oscillation (SNAO) between 1700 and 2000 CE. For this reason, in section 6, we compare the integrated paleoflood series with the atmospheric variability of simulated PCA scores of the SNAO and OMEGA configuration, and with TSI (total solar irradiance; Steinhilber et al., 2009).

6. Simulation of atmospheric variability and flood periods

Flood events from 1871 to 2010 CE show a seasonal distribution in the Swiss Alps, with the highest frequencies occurring during the summer season (Röthlisberger, 1991; Pfister, 1999; Schmocker-Fackel and Naef, 2010a; Peña et al., 2015). During July and August, the North Atlantic and Western Europe are strongly influenced by the principal year-to-year atmospheric variability pattern of the Summer North Atlantic Oscillation (SNAO; Hurrell et al., 2003; Folland et al., 2009). This variability is defined as the main empirical orthogonal function of the standardized anomalies of mean sea level pressure in the North Atlantic-European sector. During positive phases of the SNAO, a strong blocking anticyclone is located between the Scandinavia Peninsula and Great Britain.

The anomalies in the integrated flood series of the Bernese Alps were compared with these variations in atmospheric pattern, simulated over the period from 1400 to 2010 CE, to investigate the influence of atmospheric variability on alpine floods. Figure 11 identifies ten major flood pulses in the alpine Aare catchments since 1400 CE. As discussed in section 5.3 above, our

flood data are mostly in agreement with the lower temperatures (T_a in Fig. 9) in Central Europe, which may also have been influenced by episodes of volcanic eruption based on records of northern hemisphere sulfate aerosol injection (Gao et al., 2008). Furthermore, five of these ten major flood pulses occurred during phases of positive SNAO, coinciding in four cases (around 1570, 1760, 1860-1880, and 1977 CE to present) with periods of increased TSI (Steinhilber et al., 2011; 1700-1720 CE with negative TSI) and negative annual temperature anomalies (around 1570, 1760, 1860-1880 CE).

The 1400 and 1820-1850 CE flood clusters occurred during negative SNAO phases and prevailed in periods of decreased TSI, with low-pressure centers over the Atlantic domain. However, the integrated flood series shows a discrete lag with regard to the timing of TSI minima of 1470 CE and 1820, whereas the geochemical floodplain proxy of the Hasli-Aare shows a clear coincidence with negative anomalies of TSI and SNAO.

Schulte et al. (2015) compared geochemical flood proxies of the sedimentary floodplain records of the Hasli-Aare basin with paleoclimate proxies, including solar activity, tree rings, $\delta^{18}O$, and ^{10}Be over the last 3,600 years. The results suggested one dominant flood pattern defined by increased flood frequency during cold periods of lower TSI and another, less frequent, pattern during warmer climate and increased TSI periods. Similar results were suggested by Peña et al. (2015) for the last stages of the Little Ice Age and the current Global Warming based on an analysis of major summer floods in Switzerland since 1800 CE. These findings have been confirmed by this present integrated study which has focused on several alpine catchments.

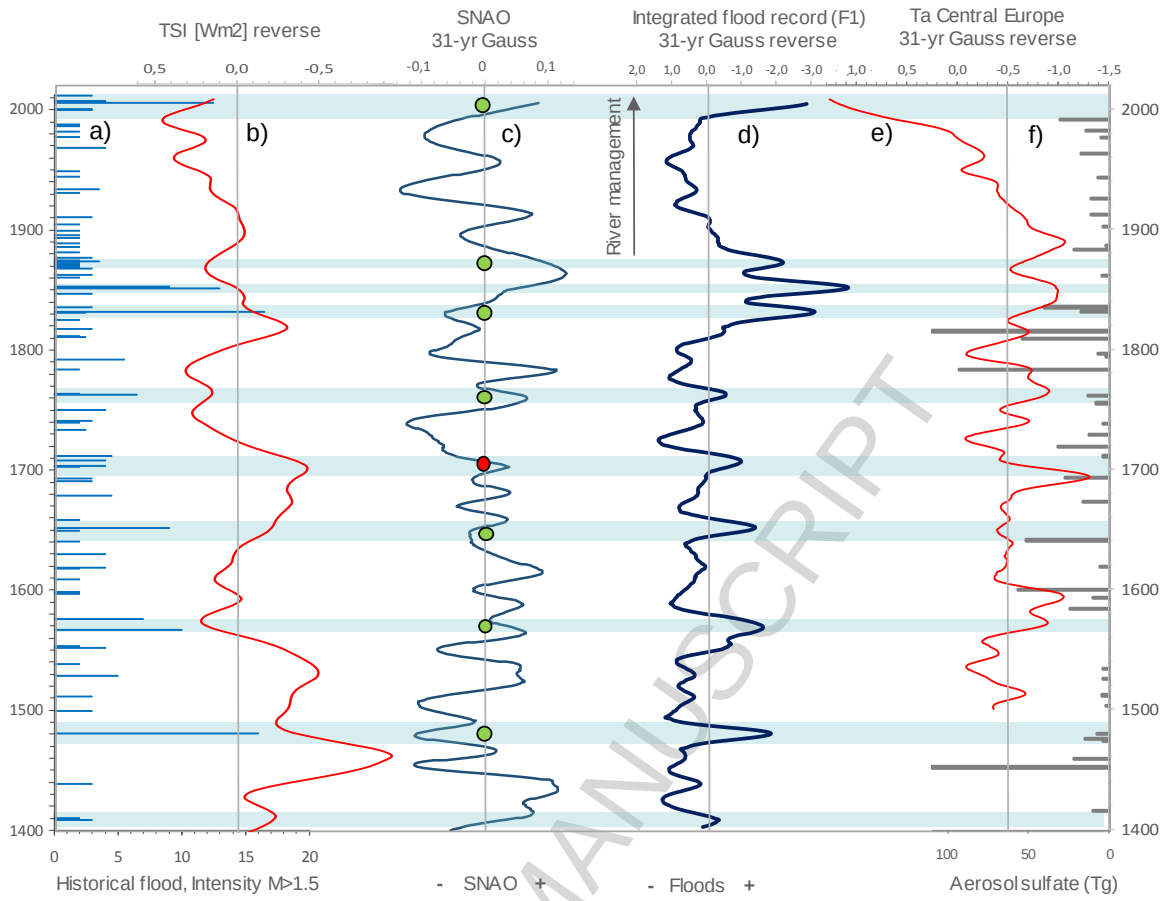

Figure 11. Correspondence between the atmospheric variability of the Summer North Atlantic Oscillation (SNAO; curve c) and the integrated flood record (d) of the Bernese Alps from 1400 to 2000 CE. Areas shaded blue are flood periods defined by the integrated flood curve. Green dots represent the correspondence between positive SNAO anomalies and positive TSI (b) during flood periods and the reverse. Red dots represent the correspondence between positive SNAO anomalies and negative TSI during flood periods and the reverse. Data series from left to right: historical floods of magnitude M>1.5 (a; this paper), Total Solar Irradiance (b; TSI, Steinhilber et al., 2009), SNAO (c), integrated flood curve (d), annual temperature of Central Europe (e; Dobrovolný et al., 2010) and annual stratospheric volcanic sulfate aerosol injection, Northern Hemisphere (f; Gao et al., 2008).

The paleoclimate simulation also reveals the emergence of individual catastrophic floods (i.e. 1566, 1762, 2005) during periods of maximum TSI (i.e. the current Global Warming) related to the positive phase of the SNAO, whose magnitudes were similar to those of the floods registered during periods of minimum TSI (i.e. 1480, 1651, 1831). Floods occurring during positive phases

of the SNAO are related to cyclones of Mediterranean origin that cross central Europe as they move north-east along the Vb track. Floods occurring during negative phases of the SNAO are associated with cold fronts originating over the Atlantic that trace a northwest to southeast passage (Peña et al., 2015).

Finally, it should be borne in mind that the relationship between floods in the Bernese Alps, the SNAO, and Central European temperatures is complex and needs further investigation (Peña and Schulte, this issue). For example, according to Figure 11, in some periods (1510-1610 and 1860-present) positive SNAO modes (July, August; 31-yr Gauss) coincided with warmer annual temperatures in Central Europe (31-yr Gauss), whereas between 1700 and 1860 lower temperature pulses were recorded during positive SNAO modes.

7 Maps of spatial flood response to specific events in the multi-archive datasets

The location and magnitude of specific past flood events were plotted in a shaded relief digital elevation model (Swisstopo; Figure 12) to study the spatial distribution of flooding in the catchments of the Bernese Alps. Here, we present two maps, which exemplify catastrophic events with different flood patterns.

The first map (top panel in Figure 12) illustrates the episode that took place between 8 and 11 July 1762 and which was the result of a 3- to 4-day persistent, intensive rainfall event, during a positive mode of the annual (JA) SNAO (2.25; cf. Figure 11), with high temperatures, and a high snow line (Röthlisberger, 1991). The simulated sea level pressure maps for 1 to 11 July (Figure 13) indicate a moist air flow in the lower troposphere turning from the

southwest (4 and 5 July 1762) to the north (5 and 6 July 1762) due to the eastward path of a low pressure system. Finally, the precipitation from 8 to 11 July 1762 was driven by an eastern flux that mainly affected the eastern sector of the Swiss Northern Alps. This precipitation before the flood episode, in combination with warmer temperatures, may have led to saturated soils, slope surface runoff, snow cover melt, high lake levels and high stream discharges, thus generating one of the severest flood events to affect the Hasli-Aare valley.

These large flood magnitudes were recorded (Figure 12) in the flood layers of Lake Grimsel; by lichenometry in the upper Hasli-Aare gorges; in historical reports of massive destruction in the village of Meiringen attributable to the Alpbach and the flooding of the entire floor of the lower Hasli valley; and by geochemical anomalies in the Eistlenbach basin. However, in the western catchments of the Bernese Alps, no flood data were recorded except for a minor flood layer in Lake Oeschinen. No data were obtained from the Lake Thun sediments as this event lay outside the range of the study undertaken by Wirth et al. (2011).

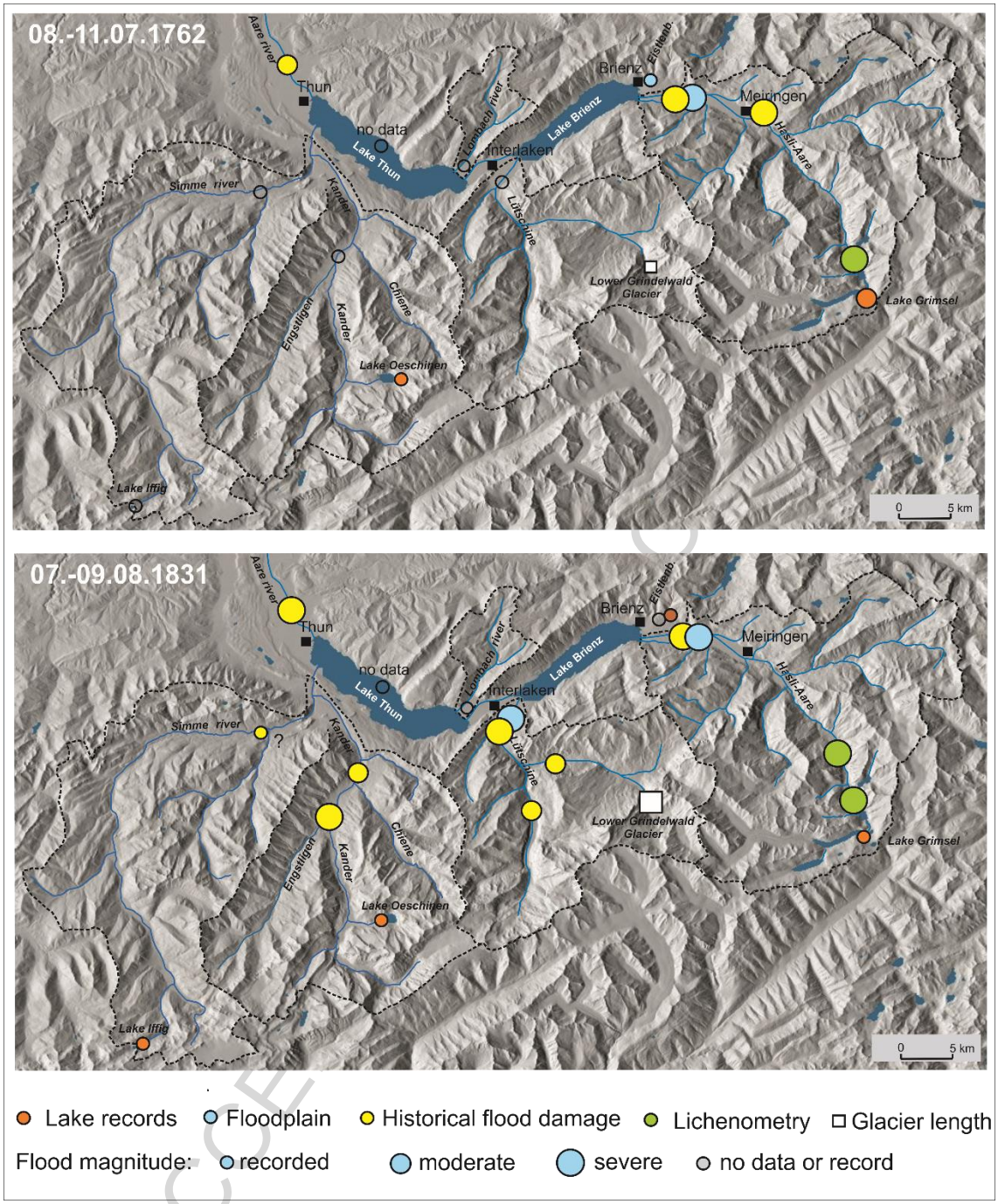

Figure 12: Spatial distribution of reconstructed flood magnitudes by flood archive type in the Bernese Alps. Maps show the flood episode from 8 to 11 July 1762 (top) and from 7 to 9 August 1831 (bottom). Shaded relief digital elevation model provided by Swisstopo (2010).

This overall picture matches the historical flood data of Röthlisberger (1991), who reconstructed severe flood damage in the eastern Swiss Cantons in the

Reuss, Limmat, Rhine and Ticino catchments. Both studies suggest that the Bernese Alps lay at the on the western edge of the precipitation field. As such, the rainfall and resulting discharges in the central and western catchments of the Bernese Alps were probably not large enough to be considered mentioning by contemporary observers of the 18th century. However, the discharge values of the Hasli Aare were of such magnitude (M = 4.5) that the floodplain between Thun and Bern was also affected by severe flooding. Interestingly, downstream of the town of Thun, documentary sources recorded damage of magnitude 2, despite the fact that the peak discharge of the Aare would probably have been buffered by the retention capacity of the two large alpine lakes of Brienz and Thun. One explanation for this is that the lakes had already reached a high level, due to a wet summer, as shown by textual documents in the case of Lake Brienz (Schulte et al., 2015) and, furthermore, as illustrated by the Swiss precipitation data of Pfister (1999), before the flood event occurred on July 8.

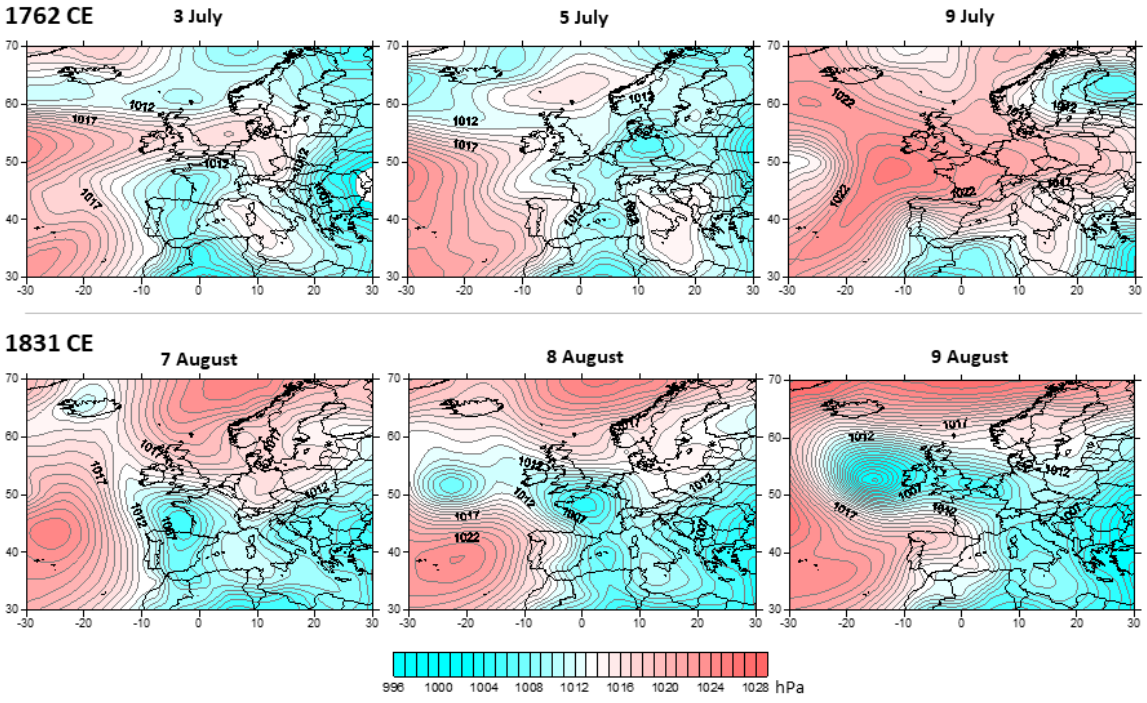

Figure 13: Composite sea level pressure (hPa) as simulated from the CESM-LME (13 runs of full forcing) for the flood episodes 8 to 11 July 1762 (top) and 7 to 9 August 1831 (bottom).

The second example of an extreme flood event in the Bernese Alps occurred between 7 and 9 August 1831 and was triggered by a two-day rainfall episode (Figure 12 and 13). The simulated SLP in Figure 13 shows the northeastward propagation of the low from the Bay of Biscay to northern France. On its eastern flank, moist, warm air masses from the Mediterranean basin were transported to the northern Alps between 7 and 8 August (Figure 13). On the third day, the Foehn wind, a warm, dry southerly wind that descends the leeward slopes of the Alps, generated additional meltwater from the snow cover and advancing glaciers (e.g. the Lower Grindelwald glacier was at its largest between 1820 and 1860) contributing to high discharges throughout the watersheds. The largest flood event in the Bernese Alps occurred during a cold climate pulse and a negative mode of the annual (JA) SNAO (-1.85; cf. Figure 11).

Almost all the archives, that is, the documentary sources, floodplain sediments, and lichenometric data, recorded extreme flooding in the higher alpine catchments (maximum elevations of 4273 m a.s.l.). This was not the case, however, of the small Eistlenbach (village of Hofstetten) and Lombach basins (floods recorded in 1752 and 1764/65). These northern tributaries are not located in the higher Swiss Alps and their elevations reach maxima of just 2085 and 2204 m a.s.l., respectively. This meant melting of snow cover during August was minor and, furthermore, precipitation intensity was, in all likelihood, lower.

The alpine lake archives show the following responses to this extreme hydrological episode: Lake Oeschinen records several discrete flood layers

around 1831 CE – flood layers of a maximum thickness of 8.9 and 9.4 mm were deposited in the interval from 1820 to 1840 CE – and, furthermore, Lakes Iffig and Grimsel also present flood pulses. However, assigning an individual flood layer to this extreme event is not straightforward given the range of dating uncertainties of these lake sequences (note that the uncertainties are greater in Lake Grimsel and Iffig sediments than in those of Lake Oeschinen).

In the broader context of the Swiss Alps, besides the Bernese Alps, the 1831 CE event also affected the Reuss catchment and the floodplain of the Rhine to the south of Lake Konstanz, according to the documentary data obtained by Röthlisberger (1991).

Finally, the most accurate estimations of flood magnitude were, we can conclude, obtained in the lower main valleys. However, there is also strong evidence from the lichen flood level records of the high Hasli-Aare catchment – and less clearly perhaps from the flood layers of the high-altitude lakes – that the 1762 and 1831 CE floods also affected the higher slopes and mountain streams of the headwater catchments. These data are essential for reconstructing the 3-D spatial pattern of large flood events.

8 Evaluation, limitations, and potential of the integrated multi-archive flood approach

The spatial-temporal integration of multi-archive flood series from the Bernese Alps provides an excellent opportunity to complete the reconstruction of the flood periods of recent centuries and to assemble multiple flood data for building a 4-D model of past flood behavior (Figure 2). However, several aspects

concerning the variation in the characteristics of the different archive types need to be given careful consideration when integrating a robust regional paleoflood time series.

The first issue that needs to be addressed is the question of the location of the flood archives in the alpine basins and what implications this might have for the flood data. This matter is especially relevant for mountain catchments because not all natural and anthropogenic flood archive types are likely to be available at all altitudes. For example, documentary flood records are most typically associated with settlements and infrastructure, which primarily occupy sites in the foreland of the Alps, on alpine valley floors and on alluvial fans (Röthlisberger, 1991; Schulte et al., 2015; Wetter, 2017). The main drawback of what are, above all, chronologically accurate records is that they extend back only a few centuries and depend on the fact of infrastructure and settlements having been exposed to flooding. Rarely do we find historical reports of flooding that do not make reference to damage to human property. However, as high-resolution floodplain sediments (Schulte et al., 2008; Laigre et al., 2013; Carvalho and Schulte, 2013) are found in the low-gradient accommodation space in the main glacial valleys, these alluvial archives are able to extend the flood series compiled from documentary sources further back in time. In our study, the flood events and periods of the Hasli-Aare, Lütschine, and Eistlenbach basins identified in the two flood series types (i.e. historic records and alluvial sediments) coincide well. Both archives report not only the same flood event but they also provide a precise tracking of the flooding processes in the floodplains and alluvial fans of the main valleys in the same area or site. The main drawback here, however, is that in recent centuries (and particularly

since the second half of the 19th century) various flood mitigation measures have been adopted, including embankments, river corrections, and reservoirs, which have modified flooding and deposition processes on the floodplains. This means that floods, and more importantly their resulting records, are increasingly being influenced by human activities and the sensitivity of these archives to extreme natural hydro-meteorological events has changed.

The location of the flood archives of lakes is likely to present greater geographic diversity than that of historical and fluvial records (Arnaud et al., 2016). Mountain flood records are often studied using lakes located in high-elevation glacial landforms (e.g. Irmler et al., 2006; Wilhelm et al., 2012; Wirth et al., 2013; Glur et al., 2013). In this study, four lakes located at altitudes ranging from 558 m a.s.l. (Lake Thun) to 2065 m a.s.l. (Lake Iffig) were included in an altitudinal transect. This use of multiple lake sites is necessary if what is sought is the reconstruction not only of local heavy precipitation events triggered by thunderstorms (i.e. local convective events) but also of larger-scale heavy precipitation events that result in major flooding of downstream areas. Thus, the question arises as to whether the records from small alpine lakes fed by catchments ranging from just several hectares to a few km^2 can be used as a proxy for larger floods, or whether their lacustrine sediments actually record the physical process of surface runoff in a small sub-catchment and so provide a better reflection of climate-environmental variability. It is for this motive that Wirth et al. (2013) and Glur et al. (2013) reconstructed flood trends in the Alps from a large number of lakes. Compiling multiple sites acts like a filter, omitting local events from the composite record. Nevertheless, our study shows that all severe basin-wide floods were recorded by one or more of the lakes (Figure 9),

with the exception of the flood period centered around 1570. Undoubtedly, the advantage of relying on alpine lakes, as opposed to the floodplains of the main valley, is that small lake catchments are not affected by flood mitigation measures and so provide continuous data down to the present day. In the case of the intensive river management that has been implemented over the last 150 years, it should be stressed that the lake flood series show great potential for providing flood proxies that can improve the sensitivity of the integrated multi-archive flood series.

A further promising approach is the one reported in recent studies undertaken in low altitude, deep, medium-sized lakes in the main alpine valleys carved out by Pleistocene glaciers (Wirth, 2011; Czymzik et al., 2013; Glur et al., 2013; Swierczynski et al., 2013; Arnaud et al., 2016; Rapuc et al., 2019, this issue). The main advantage of these deep lakes is that they trap flood deposits from the whole of the catchment. The present paper has shown good coincidence between the flood damage caused by the Kander River, discharge measurements and Lake Thun's flood layers. Their main drawback, however, is the typically high sedimentation rates of these clastic-dominated lakes, which mean complex coring logistics are required to recover long records.

A second problem to emerge is the lack of homogeneity of flood environments and their data. Apart from the difficulty of correlating and comparing flood series obtained using different dating methods with their different age uncertainties (e.g. radiocarbon, ^{210}Pb and ^{137}Cs-dating, varve counting, documentary dates, etc.), problems arise from the heterogeneity of catchments and landscapes whose hydrological and environmental settings differ (Weingartner et al., 2003). This is a fundamental concern because in many studies the flood locations that

can be inferred from natural paleoflood archives, historical sources, and instrumental flood data do not coincide geographically and so log neither the same river stretch nor the same catchment. This means more often than not having to fall back on the principle of “as close as possible”, but the resulting ‘calibration’ is, in effect, no more than a statistical correlation between different processes occurring at different sites. This is clearly a critical concern because regional studies (Glaser, 2001; Böhm and Wetzel, 2006; Schmocker-Fackel and Naef, 2010a) conclude that even neighboring catchments can present different flood responses to the same meteorological event or climatological episode, given that they are heavily influenced by a multitude of factors, including, for example, the spatial-temporal pattern of rainfall, snowline and snowmelt, water-saturated or frozen soils, land-cover, sediment and discharge contribution from glaciers, etc.

Although the density of flood archives in the Bernese Alps is high (here, in each of the catchments two or more flood archives have been analyzed), in the study reported here we have, at times, had to contend with this problem. For example, during some periods (e.g. from 1250 to 1350 CE and during the 19th century) the flood series of Lake Oeschinen presented certain differences with those of Lakes Iffig and Grimsel. The reasons for these deviations can be examined either by statistical approaches (e.g. using different thresholds and by filtering), by calibration with documentary and lake data from the same catchment (e.g. Kander River and Lake Thun) or by comparison with the flood archives of neighboring catchments (e.g. documentary data from the Aare, Lütschine and Hasli-Aare and sedimentary floodplain series). This is where the advantages afforded by the regional integration approach become effective. Maps of the

distribution of the floods recorded can shed light on the spatial pattern of flood anomalies (section 7). Because the Lake Oeschinen record could be dated with some precision, this is chosen for discussion below because problems of dating uncertainty are unlikely (Amann et al., 2015). However, other factors controlling processes such as system sensitivity (e.g. lithology resistant to erosion, runoff on steep slopes and detritus yield during minor precipitation events and increased glacier melt) and the characteristics of climatological and hydrological events (e.g. distribution and intensity of precipitation and the size of its field in combination with snow cover) need to be discussed to explain exceptional trends.

Thus, the criteria for opting to integrate or reject a particular flood data series should not only follow statistical protocols (e.g. data density and dating uncertainties) but also consider process-based arguments. Attention should be paid as to whether the records were directly affected by the physical process of river flooding. For example, infrastructure damage, river flood deposited sediments, lichen colonization of rock surfaces after flood impact, tree impacts identified by dendromorphology, among others, reflect the river dynamics during extreme events. Other compiled data, such as the lake sediments from small catchments, provide a better reflection of hydro-meteorological events. In this context, the definition of a study's aims becomes fundamental. Is the purpose to address flood risks and their impact on society or is it to provide a better understanding of climate and precipitation variability? Having said that, in many case studies it is not so easy to separate the two goals: first, because they are closely connected and, second, because many flood series provide mixed signals of different processes.

A third problem to consider is the difficulty of identifying “false alarms” and “missed” floods, especially when the study focuses specifically on individual flood events (and not on flood trends). Data series should be corroborated using known extreme hydrological events that are recorded in one or more archives. However, here, when documentary data and flood layers from lakes were compared to discharge measurements and climatological data, several mismatches were detected (section 4.4). Not all floods documented in textual or instrumental records were recorded in the natural archives. A similar picture emerges when comparing floodplain geochemical proxies with documentary and instrumental data in the lower Hasli-Aare. Yet, a study of natural flood archives also showed that these archives can record hydrological events (and, as such, serve as a useful complement to flood series) that were not recorded by documentary flood data (for example the Lake Oeschinen and Hasli-Aare floodplains), particularly before 1850 CE.

The fourth problem concerns the integration of flood data and data resolution. Here, the regional composite flood curve was generated employing a complex integration process that involved data selection, normalization, and filtering to homogenize the different series. Then depending on the structure of each series (data density, temporal resolution, and range of uncertainties), factor analysis with different settings (data series, thresholds, filtering, and smoothing) was performed to develop an integrated master flood curve that shows trends and defines flood periods. Based on the results obtained, we believe that the integration of multi-archive flood data series, such as that described herein for the Bernese Alps, is not possible with an intra-decadal or annual resolution.

The final concern is related to the applicability of results. When the integration was run with a 31-yr Gauss smoothing, we were able to define ten flood periods since 1400 CE. These could then be compared with the variations in atmospheric patterns simulated in the period between 1400 and 2010 CE (Peña and Schulte, this issue) in order to investigate the influence of atmospheric variability on alpine floods in the Bernese Alps. The relationship between the atmospheric variability of the Summer North Atlantic Oscillation (SNAO) and the integrated flood record of the Bernese Alps from 1400 to 2000 CE seem to confirm the results obtained by Peña et al. (2015) for the period 1800 to 2009 CE for all Swiss catchments. This demonstrates that even if limitations and uncertainties exist when establishing flood reconstructions (see discussion above), the integrated flood pattern agrees with our understanding of atmospheric circulation, thus highlighting the value of flood archives.

An additional field of application is the spatial integration of flood data. Using the data series from the different flood archives, maps of the most catastrophic past flood events were compiled (Figure 2 and 12). The 3-D presentation of the location and magnitude of alpine floods also incorporates those flood data that cannot be integrated into the regional synthetic paleoflood curve. The spatial reconstructions of the 1762 and 1831 CE flood events provide details as to which catchments were affected, the possible limits of the precipitation fields and the occurrence of flooding in high altitude headwater catchments (influence of temperature on type of precipitation and snowline). Moreover, this spatial information can be compared to atmospheric circulation patterns to investigate flood mechanisms and climate forcing (Figure 13).

Finally, we believe that this type of spatial analysis can be applied to most historical flood events (the next step in our ongoing work) to produce a comprehensive 4-D (temporal and spatial) flood model that includes the variability and forcing of floods in the densely populated Bernese Alps. Here, our study has shown the potential of multi-archive natural flood proxy integration at a low resolution for development over millennia time scales. However, a millennia-long series of this type would necessarily exclude documentary data since systematic textual flood descriptions are only available for this study area since 1400 CE.

9 Concluding remarks and outlook

The spatial and temporal integration of multi-archive flood series from the Bernese Alps constitutes an innovative approach to the reconstruction of accurate flood pulses over the last six centuries and the development of a temporal-spatial model of past flood behavior.

Paleoflood records from floodplains (four flood series) and lake sediments (four series), combined with documentary data (six series), were analyzed and compared with instrumental measurements (four series) and profiles of lichenometric-dated flood heights (four series) to i) determine common flood pulses (ten pulses since 1400 CE), ii) identify records which are out-of-phase and iii) investigate the sensitivity of the different natural archives. Asynchronous flood response across the sites is attributed to differences in their local hydrological regimes, influenced by (i) their physiographic parameters, including size, altitude, storage capacity and connectivity of basins, and (ii) their climate parameters, including type, spatial distribution, duration, and intensity of

precipitation. The most accurate, continuous series, corresponding to the period from 1400 to 2005 CE, were integrated into a synthetic flood master curve that defines ten dominant flood pulses around 1410, 1480, 1570, 1650, 1710, 1760, 1830, 1850, 1870, and 2005 CE. Six of these correspond to cooler climate pulses, three to intermediate temperatures, while the most recent corresponds to the current pulse of Global Warming. Furthermore, five of the ten coincide with the positive mode of the SNAO, characterized by a strong blocking anticyclone between the Scandinavia Peninsula and Great Britain.

For two of the most catastrophic flood events in the Bernese Alps (those of 1762 and 1831 CE), the location and magnitude of all the flood records compiled were plotted to provide an accurate mapping of the spatial pattern of flooding. The application of the spatial-temporal analysis developed herein to all available past flood data for integrated (or specific) flood periods and the comparison of the patterns of atmospheric variability should facilitate an in-depth understanding of the floods and of flood forcing in the catchments of the Bernese Alps. We believe that this new methodology can be usefully transferred to other mountain regions. However, as the development of a dense data network of multiple paleoflood archives is time consuming, we propose that this approach be applied in catchments where a high number of paleoflood records already exists.

Acknowledgments

The work of the FluvAlps Research Group (PaleoRisk; 2014 SGR 507) was funded by the Catalan Institution for Research and Advanced Studies (ICREA Academia 2011) and the Spanish Ministry of Education and Science (CGL2016-

75475/R). Discharge readings for the upper Aare River taken at the Brienzwiler gauging station were obtained from the BAFU (Swiss Federal Office for the Environment). Instrumental precipitation records were downloaded from the IDAWEB database (MeteoSwiss). The Swiss Federal Institute for Forest, Snow and Landscape Research (WSL) provided the flood damage data for the period 1972–2010. We gratefully acknowledge the collaboration of local government and property owners for obtaining drilling permits. Furthermore, we thank Heinz Veit (University of Bern) and Josep C. Balasch (University of Lleida) for reviewing the entire manuscript and for their helpful suggestions for improving the paper. The authors are members of the Past Climate Change (PAGES) Floods Working Group (2016-2018 and 2019-2021).

References

Amann, B., Sönke, S., Grosjean, M., 2015. A millennial-long record of warm season precipitation and flood frequency for the Northwestern Alps inferred from varved lake sediments: implications for the future. Quaternary Sci. Rev. 115, 89–100.

Amengual, A., Homar, V., Romero, R., Alonso, S. and Ramis, C., 2012. A statistical adjustment of regional climate model outputs to local scales: application to Platja de Palma, Spain. Journal of Climate 25(3), 939–957.

Armstrong, R., Bradwell, T., 2016. Growth of crustose lichens: a review. Geografiska Annaler, Series A, Physical Geography 92, 3-17.

Arnaud, F., Poulenard, J., Giguet-Covex, C., Wilhelm, B., Révillon, S., Jenny, J. P., … Sabatier, P., 2016. Erosion under climate and human pressures: An alpine lake sediment perspective. Quaternary Science Reviews, 152, 1–18.

Baker, V. R., 2008. Paleoflood hydrology: Origin, progress, prospects. Geomorphology 101(1), 1–13.

Beeli, P. 1998. Der Lauf der Aare bei Meinried. Historisch-geographische Rekonstruktion. Lizentiatsarbeit. Philosophisch-historische Fakultät, WSU, Berne.

Berner, Z.A., Bleeck-Schmidt, S., Stübena, D., Neumanna, T., Fuchs, M., Lehmann, M., 2012. Floodplain deposits: A geochemical archive of flood

history – A case study on the River Rhine, Germany. Applied Geochemistry 27(3), 543-561.

Böhm, O., Wetzel, K.-F., 2006. Flood history of the Danube tributaries Lech and Isar in the Alpine foreland of Germany. Hydrological Sciences Journal 51 (5), 784-798.

Brönnimann, S., Rohr, C., Stucki, P., Summermatter, S., Bandhauer, M., Barton, Y., Fischer, A., Froidevaux, P., Germann, U., Grosjean, M., Hupfer, F., Ingold, K., Isotta, F., Keiler, M., Martius, O., Messmer, M., Mülchi, R., Panziera, L., Pfister, L., Raible, C.C., Reist, T., Rössler, O., Röthlisberger, V., Scherrer, S., Weingartner, R., Zappa, M., Zimmermann, M., Zischg, A.P., 2018. 1868 – the flood that changed Switzerland: Causes, consequences and lessons for the future. Geographica Bernensia G94, 52 pp.

Büntgen, U., Tegel, W., Nicolussi, K., McCormick, M., Frank, D., Trouet, V., Kaplan, J.O., Herzig, F., Heussner, K.-U., Wanner, H., Luterbacher, J., Esper, J., 2011. 2500 years of European climate variability and human susceptibility, Science 331, 578–82.

Bütschi, D., 2008. Die Geschichte eines Flusses und „seiner" Menschen (1800-1950). Lizentiatsarbeit in Schweizer Geschichte, Philosophisch-historische Fakultät, Universität Bern, WSU, Bern.

Cabrera-Medin, P., Schulte, L., Carvalho, F., Peña, J.C., García, C., 2016. The influence of snow cover on alpine floods reconstructed from the analysis of satellite images. The case of the Hasli-Aare river basin, Berner Oberland (1987-2012). Geophysical Research Abstracts 18, EGU2016-9751.

Carvalho, F., Schulte, L., 2013. Morphological control on sedimentation rates and patterns of delta floodplains in the Swiss Alps. Geomorphology 198, 163-176.

Compo, G.P., Whitaker, J.S., Sardeshmukh, P.D., Matsui, N., Allan, R.J., Yin, X., Gleason, B.E., Vose, R.S., Rutledge, G., Bessemoulin, P., Brönnimann, S., Brunet, M., Crouthamel, R.I., Grant, A.N., Groisman, P.Y., Jones, P.D., Kruk, M., Kruger, A.C., Marshall, G.J., Maugeri, M., Mok, H.Y., Nordli, Ø., Ross, T.F., Trigo, R.M., Wang, X.L., Woodruff, S.D., Worley, S.J., 2011. The Twentieth Century Reanalysis Project. Quarterly J. Roy. Meteorol. Soc. 137, 1-28.

Corella, J., Valero-Garcés, B., Vicente-Serrano, S., Brauer, A., Benito, G., 2016. Three millennia of heavy rainfalls in Western Mediterranean: Frequency, seasonality and atmospheric drivers. Scientific Reports 6, 38206.

Czymzik, M., Brauer, A., Dulski, P., Plessen, B., Naumann, R., Grafenstein U. von, Scheffler, R., 2013. Orbital and solar forcing of shifts in Mid- to Late Holocene flood intensity from varved sediments of pre-alpine Lake Ammersee (southern Germany). Quaternary Science Reviews 61, 96–110.

Delaygue, G., Bard, E., 2011. An Antarctic view of Beryllium-10 and solar activity for the past millennium. Climate Dynamics 36 (11–12), 2201–2218.

Dobrovolný, P., Moberg, A., Brázdil, R., Pfister, C., Glaser, R., Wilson, R., Engelen, A. van, Limanówka, D., Kiss, A., Halíčková, M., Macková, J., Riemann, D., Luterbacher, J., Böhm, R., 2010. Monthly, seasonal and annual temperature reconstructions for Central Europe derived from documentary evidence and instrumental records since AD 1500. Climatic Change 101 (1-2), 69-107.

Dufour, G.-H., 1845-1965. Topographische Karte der Schweiz. Eidgenössisches Topographisches Bureau, Genève.

Ebersbach, R., Hoyer, W., Zahnd, E., 2010. Ein "Repräsentatives Inventar" für den Kanton Bern? Archäologie Bern 2010, Bern, Switzerland, pp. 249-271.

Folland, C. K., Knight, J., Linderholm, H. W., Fereday, D., Ineson, S., and Hurrell, J. W., 2009. The summer North Atlantic Oscillation: past, present, and future. J. Climate 22, 1082–1103.

Gao, C., Robock, A., Ammann, C., 2008. Volcanic forcing of climate over the past 1500 years: An improved ice core-based index for climate models. Journal of Geophysical Research, 113, D23111, doi:10.1029/2008JD010239.

Gees, A., 1997. Analyse historischer und seltener Hochwasser in der Schweiz: Bedeutung für das Bemessungshochwasser. Geographica Bernensia G53, Bern, Switzerland.

Gilli, A., Anselmetti, F.S., Glur, L., Wirth, S.B., 2013. Lake sediments as archives of recurrence rates and intensities of past flood events. In: Schneuwly-Bollschweiler, M., Stoffel, M., Rudolf-Miklau, F. (Eds.), Dating torrential processes on fans and cones. Methods and their application for hazard and risk assessment. Advances in Global Change Research vol. 47, Springer Netherlands, Heidelberg, Germany, pp. 225–242.

Glaser, R., 2001. Klimageschichte Mitteleuropas. 1000 Jahre Wetter, Klima, Katastrophen, Wissenschaftliche Buchgesellschaft Darmstadt, Darmstadt.

Glur, L., Wirth, S.B., Büntgen, U., Gilli, A., Haug, G.H., Schär, C., Beer, J., Anselmetti, F.S., 2013. Frequent floods in the European Alps coincide with cooler periods of the past 2500 years. Scientific Reports 3, 2770, doi:10.1038/srep02770, 2013.

Graf, M., 1991. Die Bändigung der Gewässer. Eine Geschichte der Flusskorrektionen in der Schweiz. Lizentiatsarbeit im Fach Schweizer Geschichte, Philosophisch-historische Fakultät, WSU, Universität Bern, Bern.

Guyard, H., Chapron, E., St-Onge, G., Anselmetti, F. S., Arnaud, F., Magand, O., Francus, P., Mélières, M.-A., 2007. High-altitude varve records of abrupt environmental changes and mining activity over the last 4000 years in the Western French Alps (Lake Bramant, Grandes Rousses Massif), Quaternary Science Reviews 26, Issues 19–21, 2644-2660.

Hurrell, J. W., Kushnir, Y., Visbeck, M., Ottersen, G., 2003. An overview of the North Atlantic Oscillation. In: Hurrell, J. W., Kushnir, Y., Ottersen, G., and

Visbeck, M. (Eds.), The North Atlantic Oscillation, Climatic Significance and Environmental Impact, AGU Geophysical Monograph134, 1–35.

Hügli, A., 2007. Aarewasser. 500 Jahre Hochwasserschutz zwischen Thun und Bern mit einem Vorwort von Christian Pfister. Ott Verlag, Bern, pp. 175.

Irmler, R., Daut, G., Mäusbacher, R., 2006. A debris flow calendar derived from sediments of lake Lago di Braies (N. Italy). Geomorphology 77 (1-2), 69-78.

Jenny J.-P., Wilhelm B., Arnaud F., Sabatier P., Giguet-Covex C., Mélo, A., Fanget B., Malet E., Ployon E., Perga M.E., 2014. A 4D sedimentological approach to reconstructing the flood frequency and intensity of the Rhône River (Lake Bourget, NW European Alps). Journal of Paleolimnology 51(4), 469-483.

Jones, A. F., Macklin, M. G., Brewer, P. A., 2012. A geochemical record of flooding on the upper River Severn, UK, during the last 3750 years. Geomorphology 179, 89-105.

Kylander, M.E., Ampel, L., Wohlfarth, B., Veres, D., 2011. High-resolution X-ray fluorescence core scanning analysis of Les Echets (France) sedimentary sequence: New insights from chemical proxies. Journal of Quaternary Science 26 (1), 109-117.

Laigre, L., Arnaud–Fassetta, G., Reynard, E., 2013. A 7300 year record of palaeohydrology in the Swiss Rhône River floodplain (Valais, Switzerland). Geomorphology and sustainability, 8th International conference (AIG) on Geomorphology, Paris, p. 371.

Lanz-Stauffer, H., Rommel, C., 1936. Rückversicherungsverband kantonal schweizerischer Feuerversicherungsanstalt, Bern.

Llorca, J., Schulte, L., Carvalho, F., 2014. Dinámica sedimentaria histórica en el valle Hasli (Alpes Suizos). In: Schnabel, S., Gómez Gutiérrez, A. (Eds.), Avances de la Geomorfología en España 2012-2014, XIII Reunión Nacional de Geomorfología, Cáceres, pp. 36-39.

Lohner, C.F.L.,1864. Chronik der Stadt Thun, 2 vol., Stiftung Schloss Thun, Thun.

Losada Gómez, J., Schulte, L., Gómez Bolea, A., 2014. Aproximación a la tasa de crecimiento de líquenes del grupo Rhizocarpon geographicum, en los Alpes Berneses orientales. In: Schnabel, S., Gómez Gutiérrez, A. (Eds.), Avances de la Geomorfología en España 2012-2014, XIII Reunión Nacional de Geomorfología, Cáceres, pp. 327-330.

Meyer, J.R., Weiss, J.H., 1796. Carte d'une partie très interessante de la Suisse. Johann Rudolf Meyer, Arau.

MeteoSchweiz, 2014. Klimareport 2014. Bundesamt für Meteorologie und Klimatologie, Zürich, 79 pp.

Mudelsee, M., Börngen, M., Tetzlaff, G., Grünewald, U., 2004. Extreme floods in Central Europe over the past 500 years: Role of cyclone pathway "Zugstrasse Vb". Journal of Geophysical Research 109, D23101.

Otto-Bliesner, B.L., Brady, E.C., Fasullo, J., Jahn, A., Landrum, L., Stevenson, S., Rosenbloom, N., Mai, A., Strand, G., 2016. Climate variability and change since 850 CE: An ensemble approach with the Community Earth System Model. Bulletin of the American Meteorological Society 97(5), 735-754.

Peña, J.C., Schulte, L., 2014. Effects of solar activities and climate variability on large floods in Switzerland. Bol. Asoc. Geóg. Españoles 65, 469-475.

Peña, J.C., Schulte, L., Badoux, A., Barriendos, M., Barrera-Escoda, A., 2015. Influence of solar forcing, climate variability and atmospheric circulation patterns on summer floods in Switzerland. Hydrology and Earth System Sciences 19, 3807-3827.

Peña, J.C., Schulte, L. A paleoclimate model of the atmospheric variability related to large summer floods in the Hasli-Aare (Swiss, Alps) from the AD 1300 to 2010. Global and Planetary Change [under review; this issue].

Pfister, C. 2006. Die Überschwemmung von 1566. In: Berner Zeiten. Berns mächtige Zeit. Das 16. Und 17. Jahrhundert neu entdeckt. Schulverlag blmv AG Stämpfli, Bern, 2006.

Pfister, C., 1999. Wetternachhersage. 500 Jahre Klimavariationen und Naturkatastrophen (1496–1995), Haupt-Verl., Bern.

Rapuc, W., Sabatier, P., Arnaud, F., Palumbo, A., Develle A.-L., Reyss, J.-L., Augustin, L., Régnier, E., Piccin, A., Chapron, E., Dumoulin, J.-P., Grafenstein, U. von, 2019. Holocene-long record of flood frequency in Southern Alps (Lake Iseo, Italy) under human and climate forcing. Global and Planetary Change 175, 160-172.

Reimer P. J., Baillie, M. G. L., Bard, E., Bayliss, A., Beck, J. W., Bertrand, C., Blackwell, P. G., Buck, C. E., Burr, G., Cutler, K. B., Damon, P. E., Edwards, R. L., Fairbanks, R. G., Friedrich, M., Guilderson, T. P., Hughen, K. A., Kromer, B., McCormac, F. G., Manning, S., Bronk Ramsey, C., Reimer, R. W., Remmele, S., Southon, J. R., Stuiver, M., Talamo, S., Taylor, F. W., van der Plicht, J., Weyhenmeyer, C. E., 2004. IntCal04 Terrestrial Radiocarbon Age Calibration, 0–26 Cal Kyr BP. Radiocarbon 46 (3), 1029-1058.

Röthlisberger, G., 1991. Chronik der Unwetterschäden in der Schweiz. WSL Bericht 330, Eidgenössische Forschungsanstalt für Wald, Schnee und Landschaft, Birmensdorf, 122 pp.

Schaer, A., 2003. Untersuchungen zum prähistorischen Bergbau im Oberhalbstein (Kanton Graubünden). Jahrbuch der Schweizerischen Gesellschaft für Ur- und Frühgeschichte, SGUF-Publikationen, Basel, 86, 7–54.

Schillereff, D.N., Chiverrell, R.C., Macdonald, N., Hooke, J.M., 2014. Flood stratigraphies in lake sediments: A review. Earth-Science Reviews 135, 17–37.

Schmocker-Fackel, P., Naef, F., 2010a. More frequent flooding? Changes in flood frequency in Switzerland since 1850. J. Hydrol. 381, 1–8.

Schmocker-Fackel, P. Naef, F., 2010b. Changes in flood frequencies in Switzerland since 1500. Hydrol. Earth Syst. Sci. 14, 1581-1594.

Schneider, M., 2010. Die Landschaftsgeschichte des Lambachkegels. Masterarbeit der Philosophisch-naturwissenschaftlichen Fakultät der Universität Bern, pp. 153.

Schulte, L., Veit, H., Burjachs, F., Julià, R., Burrull, R., 2004. Dinámica fluvial y variabilidad climática en los Alpes suizos durante el Holoceno superior. In: Benito, G., Díez Herrero, A. (Eds.), Actas de la VIII Reunión Nacional de Geomorfología. Sociedad Española de Geomorfología, Madrid, pp. 171-182.

Schulte, L., Julià, R., Oliva, M., Burjachs, F., Veit, H., Carvalho, F., 2008. Sensitivity of Alpine fluvial environments in the Swiss Alps to climate forcing during the Late Holocene. Sediment Dynamics in Changing Environments, IAHS Publ. 325, 367-374.

Schulte, L., Veit, H., Burjachs, F., Julià, R., 2009a. Lütschine fan delta response to climate variability and land use in the Bernese Alps during the last 2400 years. Geomorphology 108, 107-121.

Schulte, L., Julià, R., Veit, H., Carvalho, F., 2009b. Do high resolution fan delta records provide a useful tool for hazard assessment in mountain regions? International Journal of Climate Change Strategies and Management 2, 197-210.

Schulte, L., Peña, J.C., Carvalho, F., Schmidt, T., Julià, R., Llorca, J., Veit, H., 2015. A 2600-year history of floods in the Bernese Alps, Switzerland: frequencies, mechanisms and climate forcing. Hydrology and Earth System Sciences 19, 3047-3072.

Schulte, L., Carvalho, F., Llorca, J., Monterrubio,G., Peña, J.C., Cabrera-Medina, P., Gómez-Bolea, A., Sánchez-García, C., 2016. Response of paleofloods to climate variability in alpine catchments of different size reconstructed from floodplain sediments. Similarities or differences? Geophysical Research Abstracts 18, EGU2016-9544-1.

Schulte, L., Schillereff, D., Santisteban, J.I., 2019. Pluridisciplinary analysis and multi-archive reconstruction of paleofloods: societal demand, challenges and progress. Global and Planetary Change 177, 225–238.

Schwörer, C., Kaltenrieder, P., Glur, L., Berlinger, M., Elbert, J., Frei, S., Gilli, A., Hafner, A., Anselmetti, F.S, Grosjean, M., Tinner, W., 2014. Holocene climate, fire and vegetation dynamics at the treeline in the Northwestern Swiss Alps. Vegetation History and Archeobotany 23(5), 479-496.

Steinhilber, F., Beer, J., Fröhlich, C., 2009. Total solar irradiance during the Holocene. Geophys. Res. Lett. 36, L19704.

Siegfried, H., 1880. Topographischer Atlas der Schweiz (Siegfriedkarte), 25 000 / 1:50 000. Eidgenössisches topographisches Bureau / Eidg. Landestopographie, Bern.

Stucki, P., Rickli, R., Brönnimann, S., Martius, O., Wanner, H., Grebner, D., Luterbacher, J., 2012. Weather patterns and hydro-climatological

precursors of extreme floods in Switzerland since 1868. Meteorologische Zeitschrift 21(6), 531-550.

Swierczynski, T., Lauterbach, S., Dulski, P., Delgado, J., Merz, B., Brauer, A., 2013. Mid-to late Holocene flood frequency changes in the northeastern Alps as recorded in varved sediments of Lake Mondsee (Upper Austria). Quat. Sci. Rev. 80, 78–90.

Vischer, D., 2003. Die Geschichte des Hochwasserschutzes in der Schweiz. Von den Anfängen bis ins 19. Jahrhundert. Berichte des BWG, Serie Wasser, Bern, 208 pp.

Wetter, O., 2017. The potential of historical hydrology in Switzerland. Hydrology and Earth System Sciences 21(11), 5781-5803.

Wetter, O., Pfister, C., Weingartner, R., Luterbacher, J., Reist, T., Trösch, J., 2011. The largest floods in the High Rhine basin since 1268 assessed from documentary and instrumental evidence. Hydrological Sciences Journal 56 (5), 733-758.

Weingartner, R., Barben, M., Spreafico M., 2003. Floods in mountain areas – an overview based on examples from Switzerland. Journal of Hydrology 282, 10–24.

Wilhelm, B., Arnaud, F., Sabatier, P., Crouzet, C., Brisset, E., Chaumillon, E., Disnar J.-R., Guiter, F., Malet, E., Reyss, J.-L., Tachikawa, K., Bard, E., Delannoy, J.J., 2012. 1400 years of extreme precipitation patterns over the Mediterranean French Alps and possible forcing mechanisms. Quaternary Research 78(1), 1–12.

Wilhelm, B., Ballesteros Canovas, J.A., Corella Aznar, J.P., Kämpf, L., Swierczynski, T., Stoffel, M., Støren, E., Toonen, W., 2018. Recent advances in paleoflood hydrology: from new archives to data compilation and analysis. Water Security 3, 1-8.

Wilhelm B., Ballesteros Canovas J.A., Macdonald N., Toonen W., Baker V., Barriendos M., Benito G., Brauer A., Corella Aznar J.P., Denniston R., Glaser R., Ionita M., Kahle M., Liu T., Luetscher M., Macklin M., Mudelsee M., Munoz S., Schulte L., St George S., Stoffel M., Wetter O., 2019. Interpreting historical, botanical, and geological evidence to aid preparations for future floods. WIREs Water. 2019;6:e1318.

Wirth, S.B., Girardclos, S., Rellstab, C., Anselmetti, F.S., 2011. The sedimentary response to a pioneer geo-engineering project: Tracking the Kander River deviation in the sediments of Lake Thun (Switzerland). Sedimentology 58 (7), 1737-1761.

Wirth, S.B., Glur, L., Gilli, A., Anselmetti, F.S., 2013. Holocene flood frequency across the Central Alps – solar forcing and evidence for variations in North Atlantic atmospheric circulation, Quaternary Science Reviews 80, 112-128.

Table joint to Figure 1: List and characteristics of the studied catchments.

Catchment	Type of archive	Catchment (km2)	Elevation record (m a.s.l.)	Highest elevation (m a.s.l.)
Lake Thun	Lake, historical	2451	558	4273
Hasli-Aare	Fluvial, hist., instr., lichen, lake Grim.	596	568	4273
Simme	Historical, instr., lake Iffig	594	663	3243
Kander	Historical, instr., lake Oes.	496	646	3698
Lütschine	Fluvial, hist., instr.	379	569	4158
Lombach	Fluvial, hist.	48	569	2085
Lake Oeschinen	Lake	21	1580	3661
Lake Grimsel	Lake	5	1908	2941
Lake Iffigsee	Lake	4,6	2065	3246
Eistlenbach	Fluvial, hist., tree rings	4	644	2204

Graphical abstract:

Highlights

- Spatial and temporal integration of paleoflood data series from floodplain sediments, lakes, documents, lichens and gauging stations
- 600-yr long synthetic multi-archive flood record of the Bernese Alps
- 6 of 10 flood periods correspond to cooler climate pulses, one period to warm climate, 5 events to +SNAO
- Paleoclimate simulation of events and mapping of past flood magnitudes
- Development of a four-dimensional paleoflood model in alpine catchments